

EROS AND FAINT RED GALAXIES

Patrick J. McCarthy

*Observatories of the Carnegie Institution of Washington, Pasadena,
California 91101; email: pmccarthy@ociw.edu*

Key Words galaxy evolution, galaxy formation, infrared surveys, starburst galaxies

■ **Abstract** This chapter reviews the properties of faint IR-selected field galaxies and the extremely red color-selected populations in particular. These populations are a mix of passively evolving stellar systems and heavily obscured star-forming galaxies. The star-forming component appears to constitute 20–50% of the population depending on the magnitude and color cuts employed. The remaining objects are a mix of passively evolving ellipticals and early-type disk galaxies. The passively evolving red galaxies are strongly clustered in space and are likely the high-mass high-luminosity end of the elliptical galaxy progenitor population at redshifts between one and two. These galaxies have masses and space densities that appear to be in conflict with late-forming hierarchical galaxy-formation models. The red galaxies appear to be a population that is distinct from the moderately star-forming Lyman-Break galaxies but may be related to the starburst population at $z > 2$ seen in deep submillimeter surveys.

1. INTRODUCTION

In the past decade a new field of galaxy research has emerged: the study of the faint red galaxies and Extremely Red Objects, or EROs. The faint red galaxies, the less-studied component of the faint field-galaxy population, have received little attention at the review level in part because the study of this population is a relatively young field. The first members of this class were not identified until 1989–1991. This chapter reviews the properties of the near-IR-selected field-galaxy population with an emphasis on those with red near-IR to optical colors. Brief reviews of this field can be found in Cimatti et al. (2003a,b).

The subject of the faint blue star-forming galaxy population has been covered in a number of volumes in this series. Ellis (1997) reviewed the *Faint Blue Galaxies* in Volume 35, Koo & Kron (1992) reviewed the *Evidence for Evolution in Faint Field Galaxy Samples* in Volume 30. The review of *The Hubble Deep Fields* by Ferguson, Dickinson & Williams (2000) in Volume 38 was focused, in large part, on the very faint field galaxy population. Giavalisco's (2002) review of *The Lyman-Break Galaxies* in Volume 40 dealt with the UV-bright component of the distant galaxy population and discussed many of the issues to be addressed in the present review, but from a different and complementary perspective.

2. DISCOVERY OF THE FAINT RED POPULATION

The red galaxy population was “discovered” over a period of a few years by a number of observers. To say that the population was recognized is a better descriptor than discovered in this context, because most of the objects in question are detectable in the visible. Their unusual properties were simply not recognized before the availability of IR-imaging detectors.

The earliest high-latitude surveys with IR focal-plane arrays revealed the red population. Elston, Rieke & Rieke (1988) surveyed an area of only 10 square arc-minutes, yet they detected two objects with colors that were redder than those expected from nominal evolutionary tracks. Elston, Rieke & Rieke (1988) recognized this as a new population but identified the red colors as a signature of the Lyman continuum break and, hence, assigned very high redshifts (e.g., ~ 6 – 25) to place the Lyman edge between the R and K bands.

Cowie et al. (1990) imaged a field of 1.6 arc-min^2 for 22 hours with the UH 2.2-m telescope. They identified a number of galaxies with $I - K \sim 5$ and suggested that these were likely to be normal galaxies $z \sim 2$. McCarthy, Persson & West (1992) identified a number of galaxies with $R - K \sim 5$ – 6 in fields centered on $z \sim 2$ radio galaxies. McCarthy et al. (1992) suggested that these red galaxies were evolved cluster members at the same redshifts as the radio galaxies. Hu & Ridgeway (1994) detected two galaxies with $I - K > 5$ from a survey of 100 square arcminutes and suggested that they were at redshifts near 2.5 as this would shift the steep rest-frame UV portion of the spectral energy distribution of a normal galaxy into the R -band.

In the early 1990s numerous other observers were detecting similar red objects in high latitude near-IR-imaging programs. In fact the surface density of red galaxies on the sky is such that they are difficult to avoid. Persson et al. (1993) detected a number of extremely red galaxies in early observations with Palomar’s IR imaging camera, as described in Soifer et al. (1999). Early large area, but fairly shallow, surveys at Calar Alto (e.g., Thompson et al. 1999a,b) characterized the bright end of the red population.

Spectroscopy, and especially redshift determinations, was slow going for the red objects. Elston, Rieke & Rieke (1989) were able to obtain redshifts for the brightest of their red galaxies. These spectra revealed the signatures of evolved stars at $z \sim 0.8$, leading them to conclude that the red objects were primarily old stellar populations at modest redshifts rather than primeval galaxies. The objects with spectroscopic redshifts measured by Elston, Rieke & Rieke (1989) were not the most extreme component, in terms of optical-to-IR color, of the red population, but one can now see that they were representative of the bright galaxies on the threshold of the $z > 1$ very red population. Graham & Dey (1996) reported a redshift of $z = 1.44$ for one of the two extremely red galaxies from the Hu & Ridgeway (1994) sample. Their redshift determination was based on the detection of broad $H\alpha$ emission using a near-IR grism spectrometer. They concluded that the object in question, called HR10 at the time, was an obscured star-forming

galaxy. Dey et al. (1999) subsequently confirmed the redshift on the basis of [OII]3727 emission. It remains the case today that redshifts for the red population are more easily obtained in the visible, because of the multiplex advantage and the higher detector performance of CCD-based spectrographs. This situation is likely to change as multiobject cryogenic spectrometers using the latest generation of low-noise large-format mosaic-like IR arrays come on-line.

These early investigations set the stage for much of the work that has followed in the ensuing decade. The essential dichotomy between old stellar populations and obscured star-forming galaxies remains a central point of discussion in this field and is a key part of the present review. Both classes of object offer the potential for insights into the formation of massive galaxies and both are significant constituents of the high redshift universe.

3. K-CORRECTIONS, EVOLUTION, AND EXTINCTION

Very red optical-to-IR colors (e.g., $R - K > 5$) arise when the spectral energy distributions of more or less normal galaxies are redshifted such that the observed-frame visible samples the steep portion of the rest-frame UV spectral energy distribution (SED) while the near-IR samples the flatter region of the rest-frame visible spectrum. The red colors have less to do with the 4000 Å break, per se, than they do with the overall steep shape of the UV spectra of normal and dusty galaxies. The observed color of a nonevolving elliptical galaxy spectrum will change from $R - K = 4$ to $R - K = 9$ over the interval from $0.7 < z < 3.4$ even though the 4000 Å break is between the R and K filters over this entire redshift range. Galaxies with rather different internal properties can have similar $R - K$ or $I - K$ colors, and indeed they can have very similar spectral shapes over the full optical-near-IR spectral range.

Figure 1 shows the observed-frame $R - K$ and $I - K$ lines for a variety of nonevolving galaxy spectral shapes. These can be constructed from the K-corrections given in Poggianti (1997) or computed using the Coleman, Wu, & Weedman (1980) template spectra. In the right panel nonevolving elliptical systems (first dashed line) cross the $I - K > 4$ line at nearly the same redshift as the early-type spirals (second dashed line). In the left panel of Figure 1 the same trajectories are plotted, but in this case a varying degree of extinction to the Sab template (second solid line from top) is added. One can see that even for fairly large amounts of reddening, redshifts near unity are still required to reach the $R - K > 5$ threshold. To first order, the red galaxies have their distinctive colors primarily because they are at redshifts near one. Thus, simple $R - K$ or $I - K$ color cuts can be quite effective in selecting high redshift galaxy samples. This color selection is not as precise as the Lyman-break technique for star-forming galaxies (Giavalisco 2002) as it employs a smoothly varying spectral *shape* rather than an edge, but it benefits from the fact that very few galaxies can have $I - K > 4$ at any redshift significantly below unity.

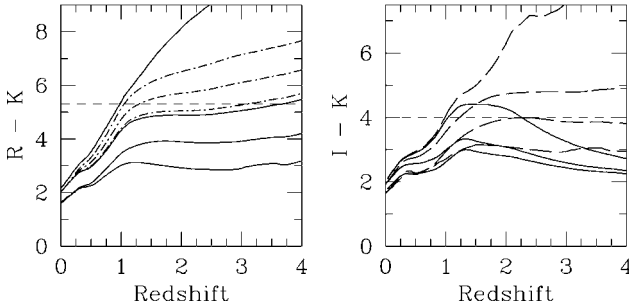


Figure 1 Observed-frame color tracks for nonevolving, evolving, and reddened galaxy models. The panel on the left shows $R - K$ for nonevolving E/S0, Sab, Scd, and Irr SEDs (from top to bottom), computed from Coleman, Wu & Weedman (1980), as solid lines. The dashed lines are the Sab SED with $A_v = 1, 1.5,$ and 2 magnitudes. The right panel shows $I - K$ for evolving models with $z_f = 30$ and decaying star formation with e-folding times of 1, 2, 3 Gyr and a constant star formation rate model. The same nonevolving SEDs from the left panel are shown in $I - K$ as dashed lines in the right panel. In each panel the nominal ERO color definition is marked with a dashed line.

Evolution does not significantly change the color at which the $z = 1$ threshold is crossed. The behavior at high redshifts, however, does change when one includes passive evolution, as galaxies do not continue to get redder beyond some fiducial redshift. The exact value of this transition redshift depends on the formation history and world model, but is < 2.5 for most plausible scenarios. Thus, whereas an $I - K$ or $R - K$ color selection will work well at $z \sim 1$, it is not effective at identifying $z > 2$ galaxies. Shifting the color selection to longer wavelengths, $J - K$ for example, allows a similar selection criterion to be applied to $z \sim 2.5$ with considerable effectiveness (Franx et al. 2003).

In addition to colors, the apparent magnitudes of red galaxies contain clues as to their nature. Figure 2 shows the expected apparent magnitude corresponding to K^* for no evolution and fixed-mass passive evolution models. For large formation redshifts (e.g., $z_f \sim 5$ to 10, the solid and dotted lines in Figure 2, respectively) and simple stellar populations, the apparent magnitude corresponding to K^* at $z = 1$ is ~ 18 ; at $z = 2$ it falls to $K \sim 20$ for very early (e.g., $z_f > 5$) formation, but remains rather bright for late-forming models. These curves provide a guide for estimating the redshift ranges probed by surveys to various depths. Shallow all-sky surveys such as the 2-Micron All Sky Survey (2MASS) do not reach $z \sim 0.5$, while very deep pencil-beam samples, such as the NICMOS Hubble Deep Field (Thompson et al. 1999) reach deep into the luminosity function (LF) to redshifts well beyond $z = 3$.

In hierarchical models, galaxies do not form in a single collapse event and so the simple stellar population tracks above are not appropriate. In hierarchical models the apparent value of K^* will fall below the passive evolution expectation, and the degree of mass evolution can be constrained from the change of K^* with redshift (e.g., Kauffmann & Charlot 1998).

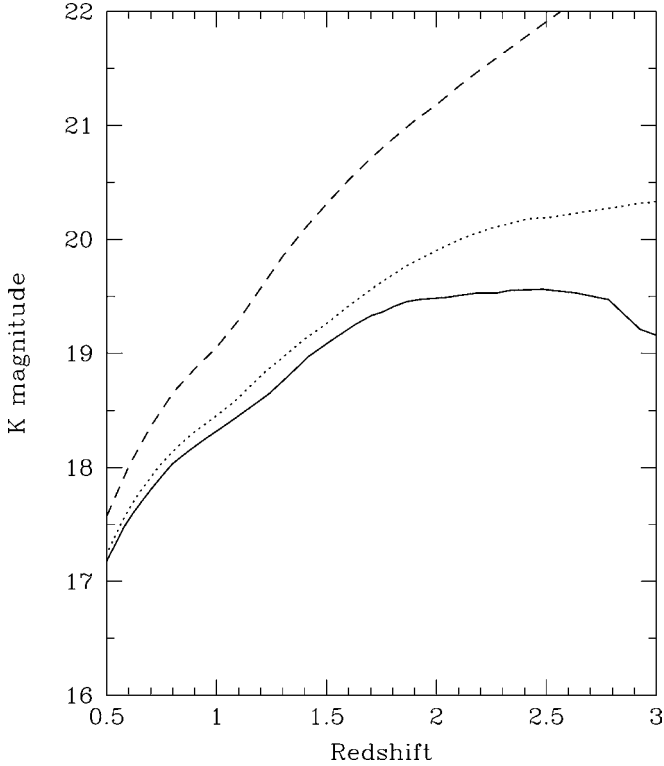


Figure 2 The apparent magnitude corresponding to K^* is plotted against redshift for no-evolution and pure luminosity evolution models. The no-evolution track is shown as a dashed line, pure luminosity evolution models with instantaneous burst at formation redshifts of 10 and 5 are shown as dotted and solid lines, respectively. This plot illustrates that surveys to $K \sim 19$ – 20 are quite sensitive to the rate of evolution in the massive galaxy population. These curves are computed for a $\Omega_m = 0.3$, $\Omega_\lambda = 0.7$, $H_o = 70$ cosmology. These cosmological parameters are used throughout the review.

4. COLOR-SYSTEMS, NOMENCLATURE, AND SKY DENSITIES

4.1. Color Systems

In this review we are primarily interested in those objects with optical-to-near-IR colors that are redder than the bulk of the faint field galaxy population. Of the standard IR band-passes defined by Johnson (1962) and updated with the use of modern detectors, such as the United Kingdom IR Telescope (UKIRT) system, the J , H , and K system (plus the K' and K_s band-passes of Wainscoat & Cowie 1992) are most relevant. Most studies of the red galaxy population are based on $R - K$ colors, some are based on $I - K$, and a few use either $R - H$ or $I - H$.

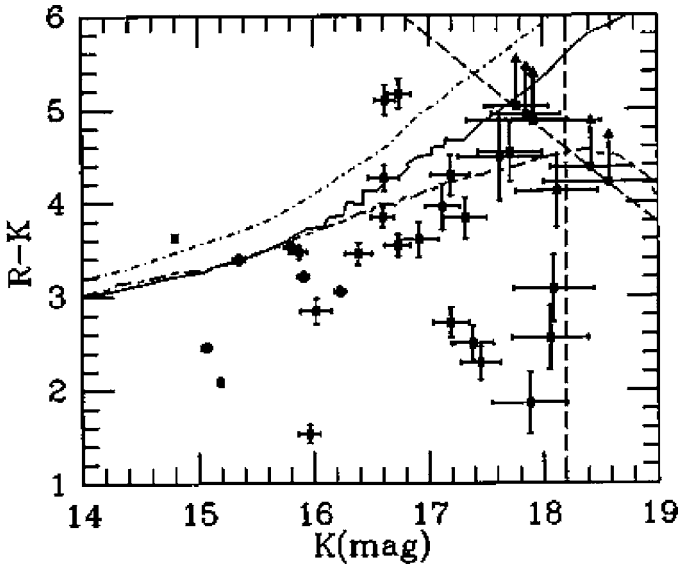


Figure 3 The $R - K$ versus K color-magnitude diagram (CMD) from Elston, Rieke & Rieke (1988). The curves show the tracks expected for no-evolution (*dot-dashed line*) and passively evolving (*solid line*) early-forming galaxies. The two objects with $R - K \sim 5$ and $K \sim 16$ stand out as being well outside the expected locus of normal galaxies.

Whereas the $R - K$ system is the more common system, $I - K$ is a preferred system. Its narrower wavelength baseline and redder optical passband allow for cleaner separation of the red population and better redshift isolation, as can be seen in Figure 1.

Figures 3 and 4 show two color-magnitude diagrams (CMDs). Figure 3 is from Elston, Rieke & Rieke (1988) and demonstrates the basics of the $R - K$ versus K CMD. The curves show the expected tracks for normal galaxies K -corrected and evolved through the filter band-passes. The two objects with $R - K > 5$ and $K \sim 16.5$ appear to lie outside of the locus of colors available to normal stellar populations. Figure 4 is a modern $R - K$ versus K CMD for comparison. This figure is from the Las Campanas IR survey (Chen et al. 2002, Firth et al. 2001, McCarthy et al. 2001); similar diagrams have been derived from a number of other programs (e.g., Cowie et al. 1990, Hu & Ridegway 1994).

4.2. Nomenclature

The red galaxies found in these near-IR surveys are now generally referred to as Extremely Red Objects, or EROs. This term was introduced by A. Dey and was intended to refer to objects with $R - K > 6$. The term is now widely used, but the

original definition is not strongly adhered to. Various authors have used the ERO term to refer to objects with $R - K > 5$ (e.g., Daddi et al. 2000), $R - K > 5.3$, (e.g., Smail et al. 1999), $R - K > 6$, or $I - K > 4$, $I - K > 5$, $I - H > 3$, and even $R - F160W > 4$. To add to the confusion some authors (Moustakas et al. 2004, Stanford et al. 2004) use color definitions (e.g., $R - K > 3.35$) in the AB system, whereas others use the combined HK' filter of the color system by Wainscoat & Cowie (1992). The ERO designation is reminiscent of the Blue Stellar Object (BSO) term used in the early days of quasar surveys. When the term was widely used it was difficult to separate QSOs from white dwarfs and hot subdwarfs and so the object designation was appropriate. Similarly, the ERO designation reflects, in part, early difficulty in separating cool stars from red galaxies in two filter imaging (e.g., R and K) data sets. Multicolor imaging surveys eventually became fairly good, but not perfect, at removing stars from QSO samples. Similarly, it is now fairly straightforward to differentiate galactic M and later-type stars from the galaxy population with the use of multiple colors. Separating different types of red galaxies (e.g., evolved stars versus reddened star bursts) is possible to a modest degree, but requires quite precise photometry. We have reached the point where the object designation is unnecessarily vague.

Several authors have introduced additional classes and labels for the red galaxies. Im et al. (2002) call objects with $R - K > 7$ Hyper-Extreme Red Objects (HEROs). Barger et al. (2003), Alexander et al. (2002), and others refer to objects with $5.3 < R - K < 6$, $4 < I - K < 5$, as Very Red Objects (VROs). Others have introduced Very Red Galaxies (VRGs) and Faint Red Outlier Galaxies (FROGs) (Moustakas et al. 1997). At this time there does not appear to be any physical basis for placing an object with an $R - K$ color of 5.9 in a different class from one with a color of 6.1. It is not even clear that galaxies with color differences as large as one magnitude are necessarily different classes of object. This arises in part because of a genuine diversity in stellar content and internal reddening and in part because of the impact of the K -correction on color. Classifying objects on the basis of their observed-frame properties is obviously fraught with danger. The original motivation for the ERO class was that there was a clean limit to the colors that normal galaxies can attain and thus one could isolate objects that were beyond this locus. The VRO designation was intended to label ordinary red galaxies, reserving ERO for extraordinary objects. The viability of this approach is not so clear at this time, particularly when based on an observed-frame color. In practice the ERO threshold is now defined by most authors as the color needed to isolate $z > 1$ red galaxies, be they old or obscured (see Figure 1). It appears then from Figure 1 that $R - K > 5.3$ and $I - K > 4$ are sensible definitions for the class, and this chapter refers to ERO to mean such, except where others have found it convenient to use different color definitions!

4.3. Surface Density on the Sky

Many of the early papers in this field dwelt on the question of how many red galaxies of a particular color and magnitude exist per unit area on the sky (e.g.,

Thompson et al. 1999a,b; Martini 2001). The discovery observations were based on such small areas that any meaningful determination of the sky density was difficult, if not impossible. As the number of surveys increased it became apparent that there were significant differences between the surface densities reported by various groups. Thompson et al. (1999a) reported a fairly low sky density, whereas Yan et al. (2000) reported a significantly higher density (~ 1000 per square degree to $H = 21.5$). Understanding the sky densities was more than just an exercise in quantifying the population. It offered a direct means of determining the space density of early-type galaxies at intermediate redshifts.

The discovery of the high degree of angular clustering in the red population was seen as a means to reconcile the wide range of reported surface densities, as discussed in Daddi et al. (2000). Whereas the clustering does have a significant impact on small and intermediate scales, it is unlikely to be the cause of all of the discrepant measurements (as shown in Chen et al. 2004). A significant source of confusion, I believe, lay in the very steep number-magnitude and color-magnitude relations for the red galaxies as shown in Figure 5. Surveys with only slightly different depths or color thresholds will correctly yield quite different sky densities.

Simple sky densities provide limited insight in the to nature of the population. Number-magnitude relations, commonly called number-counts, provide a statistical probe of both the 3-space distribution of the population and its evolution. McCarthy et al. (2001), Firth et al. (2001), and Smith et al. (2002) derived number-counts as a function of color for various red samples. The combined Las Campanas Infrared Survey (LCIR) and Yan et al. (2000) samples shown in McCarthy et al. (2001) revealed a flattening of the red counts at $H \sim 20$. Smith et al. (2002) used observations of sources lensed by a foreground cluster to extend the counts for K -selected red galaxies to $K \sim 21.5$. Smith et al. combined their deep sample with larger area K -band samples from Daddi et al. (2000), and Thompson et al. (1999) and inferred a break in the slope of the counts at $K \sim 19$, very similar to the break seen in the $I - H$ counts in McCarthy et al. (2001). Wehner et al. (2002) also used gravitationally amplified fields to infer the faint red counts. Their red galaxy counts appear to be biased by a particularly rich sightline as their counts imply that 30–50% of the population at $K \sim 18.5$ have $I - K > 4$, in conflict with many other results. This illustrates the limitations of lensing as a probe of a highly clustered population (also see Takata et al. 2003).

Figure 5 shows number magnitude relations for K -band selected samples. The slope of the full K -selected counts, $d(\log(N))/dm$, is 0.26 (Djorgovski et al. 1995, Gardner et al. 1996, Huang et al. 2001, Moustakas et al. 1997, Yan et al. 1998). The lower curves show the counts for various color cuts ($R - K > 5.3$ and 6.0 on the right and $I - K > 4, 4.5, 5, 5.5$ on the left). The counts for even moderately red color cuts are quite steep: The slope of the counts for $I - K > 4$ in the range $17 < K < 20$ is 0.9 ± 0.1 , roughly three times steeper than the full K sample. At bright magnitudes (e.g., $K \sim 17$) the red galaxies comprise a tiny fraction ($\sim 2\%$) of the total field population, whereas at $K \sim 20$ 10–15% of the objects

have $I - K > 4$ or $R - K > 5$. As we saw in Figure 1, simple color cuts in $R - K$ or $I - K$ can effectively remove the $z < 1$ foreground from galaxy surveys. This observation and the steep slope of the red galaxy counts are closely related. The steep slope of the counts at relatively bright magnitudes reflects the exponential cutoff of the galaxy luminosity function. Unlike the full K -selected counts, the red color-selected objects span a fairly narrow redshift range, and thus the shape of the counts more closely reflects the shape of the luminosity function rather than the three-space distribution. The flattening of the red counts can be understood as the result of transitioning from the exponential cutoff of the luminosity function to a flatter region and hence a transition from the counts sampling primarily the LF to a sampling of the volume. The differential counts, while requiring larger samples, are a more sensitive probe of changes in slope at faint magnitudes than the cumulative counts shown on the right.

The counts are also a steep function of color. Increasing the color cut from $I - K > 4$ to $I - K > 5$ reduces the counts by nearly a factor of ten. The break in the slope of the counts moves to fainter magnitudes as one transitions to redder colors. Redder colors sample high redshifts and push K^* to fainter magnitudes and hence the break in the counts moves from $K = 19$ for $I - K = 4$ to $K \sim 19.7$ for $I - K = 5$. Similar behavior can be seen in the $R - K$ selected counts in Smith et al. (2002) who show that pure luminosity evolution (PLE) models provide a good match to the observed cumulative counts for $R - K > 5.3$ and $R - K > 6$.

It is now clear that not all of the red galaxies are passively evolving systems and so the conceptual picture of the red counts outlined above is a simplification. The steep drop in surface density as a function of color reflects some combination of the increase in z_{min} with increasing color and the rarity of objects with spectral slopes steep enough to produce the reddest colors (e.g., $R - K > 7$) at any redshift. There are reasons to believe that heavily reddened systems make an increasing contribution to the counts both at faint magnitudes and particularly in the reddest colors (e.g., Smail et al. 2002).

5. THE NATURE OF THE RED GALAXIES

The red galaxies were first suspected of being the classical primeval galaxy population at very high redshift. It was not long before this was seen to be too good to be true, and it was suggested that the red population lay primarily in the $2 < z < 3$ range (e.g., Cowie et al. 1990, Hu & Ridegway 1994, McCarthy et al. 1992), also an optimistic estimate. It is now fairly well demonstrated that the bulk of the red population lies between $1 < z < 2$ with a tail of the most extreme reddened starbursts to somewhat higher redshifts. The redshift determination for HR10 by Graham & Dey (1996), their identification of it as a dusty star-forming galaxy, and the subsequent confirmation of this via submillimeter observations (Cimatti et al. 1998, Dey et al. 1999) showed clearly that spectroscopy of the red galaxies would yield more than simple redshift determinations. The basic dichotomy

between evolved systems and dusty starbursts remains one of the central questions in the study of these objects. Understanding the balance of the two types of systems, if indeed they can be divided so simply, is essential before one can make sense of many of the statistical properties of the population. Space densities, luminosity functions, and clustering strengths, to name just a few, are difficult to interpret if the parent population is composed of two classes of systems with nearly diametrically opposed properties. That the mix of old versus dusty systems may be a strong function of color, magnitude, and redshift serves to further cloud the situation.

5.1. Far-IR, Submillimeter, and Centimeter-Wave Emission

Cimatti et al. (1998) and Dey et al. (1999) showed that the rest-frame properties of HR10 are broadly consistent with that of Arp 220, the prototypical ultraluminous IR galaxy (e.g., Rieke et al. 1985). Elbaz et al. (2002) made a strong case for HR10 being a distant clone of Arp 220, scaled by a factor of approximately four. A large mass ($\sim 10^{11} M_{\odot}$) of molecular gas has been detected in this object (Andreani et al. 2000; Greve, Ivison & Papadopoulos 2003) further cementing its place as the prototypical ERO starburst galaxy.

The spectacular nature of HR10 led to a number of other attempts to detect red $R - K$ or $I - K$ selected objects at submillimeter wavelengths with the Submillimeter Common-User Bolometer Array (SCUBA) (Holland et al. 1999) on the James Clerk Maxwell Telescope (JCMT). Few of these targeted searches have resulted in detections. Mohan et al. (2002) report a deep submillimeter and centimeter-band radio search for emission from EROs with $K < 20$. Only 1 in 14 of the $I - K > 5$ objects was detected at submillimeter wavelengths and only two were detected at 1.4 GHz. The color cut used by Mohan et al. is clearly in the “extremely red” territory rather than simply “very red” and yet their detection rate in the submillimeter is less than 10%. By stacking images of all of their nondetections they derived an upper limit to the 850 μm flux density of 1.0 ± 0.12 mJy (0.18 ± 0.12 at 1250 μm). This upper limit translates to a star-formation rate of less than $\sim 500 M_{\odot} \text{yr}^{-1}$ for $z = 1.5$. This is not a terribly restrictive limit. Wehner et al. (2002) carried out a similar analysis, but focused on gravitationally lensed fields behind rich clusters of galaxies. They reported a significant detection of a mean signal from their stacked image of objects with $I - K > 4$, $K < 21.4$, somewhat fainter, but not as extreme in color as the Mohan et al. sample. The mean 850 μm flux density reported by Wehner et al. (2002) (1.58 ± 0.13 mJy) is 50% higher than the upper limit reported by Mohan and only a factor of three below the HR10 flux density reported by Dey et al. It is of interest to note that Wehner et al. report a mean 850 μm flux density for objects with $3.5 < I - K < 4$ that is not much different from that of the $I - K > 4$ objects. They estimate that $\sim 50\%$ of the integrated 850 μm background can be attributed to galaxies with colors redder than $I - K = 3.5$. Far-IR observations with the Spitzer Infrared Telescope Facility will likely have tested this before this volume goes to press.

Smail et al. (1999) imaged a number of SCUBA cluster lensing survey fields in the visible and near-IR. Identifications based on the SCUBA positions alone are scarce and often unreliable, as the beam size at $850\ \mu\text{m}$ is $15''$. Smail et al. (1999, 2002) used deep Very Large Array (VLA) observations to obtain precise source positions at 20 cm, as a large fraction of the submillimeter sources are also detected at 20 cm. The radio-far-IR correlation, in essence, allows one to use centimeter wavelengths as a proxy for the submillimeter source population (Barger, Cowie & Richards 2000; Carilli & Yun 2000; Yun & Carilli 2002). Smail et al. (1999) found that two of their SCUBA/VLA sources were coincident with objects having truly extreme colors ($I - K > 6$) and fairly bright K magnitudes. The $850\ \mu\text{m}$ flux densities of these sources are quite a bit larger than HR10 and Smail et al. (1999) infer from the $850\ \mu\text{m}$ to 1.4 GHz flux ratio that the two sources lie at $z > 2$ and $z > 4$, respectively. These objects may well represent the best examples of very high redshift heavily obscured starbursts associated with EROs.

Smail et al. (2002) made use of the connection between submillimeter and centimeter-wave emission in a deep multiwavelength study of a modest area field. Approximately one third of objects with $R - K > 5.3$ and $K < 20.5$ are detected at 1.4 GHz with flux densities greater than $12.5\ \mu\text{Jy}$. Adopting a typical redshift of ~ 1 , Smail et al. (2002) estimate that the observed radio flux densities correspond to star-formation rates of $\sim 25\ M_{\odot}\ \text{yr}^{-1}$ in massive stars alone. About one third of these radio sources are resolved and hence are not Active Galactic Nuclei (AGN) dominated. The relatively low resolution of the radio observations is such that many disk galaxies would not be resolved and thus a large fraction of the radio sources are probably powered by star formation rather than nuclear point sources. Smail et al. (2002) make a case for 30–60% of the $K < 20.5$ red population arising from dusty star-forming galaxies.

Afonso et al. (2003) examined the radio properties of EROs in the Phoenix radio survey. Whereas Afonso et al. (2003) detected few ($\sim 5\%$ of the sample) individual red galaxies in their radio images, they did detect a significant signal from a stacked map of nondetected $R - K > 5$ galaxies. This signal corresponds to a mean star-formation rate of $61\ M_{\odot}\ \text{yr}^{-1}$, if all of the radio emission is associated with star formation and supernovae (SNe).

The prototypical evolved red galaxy, 53W091, is a weak radio source from the Leiden-Berkeley Deep Survey (LBDS) (Windhorst et al. 1984). The LBDS sources are a mix of low-redshift star-forming galaxies and low-to-intermediate redshift AGN. The classical radio galaxies (e.g., 3CRR,B2/1Jy,MRC,4C) often have host galaxies with very red optical to near-IR colors. Much of the science that is now being carried out or contemplated with the evolved red field galaxies was attempted with the classical radio galaxies in past decades. Lilly & Longair (1984) argued that the colors and K -band *Hubble* diagram of the Third Cambridge Revised-Revised (3CRR) (Laing, Riley & Longair 1983) sample implied a common large-formation redshift for the radio galaxy hosts. Dunlop et al. (1989) carried out a similar analysis of sources in the Parkes Selected Regions. The realization that the central AGN has a close connection to the rest-frame UV in powerful radio

galaxies (see McCarthy 1992 for a review) tempered interest in using radio galaxies as probes of either cosmology or galaxy evolution. The dismissal of the 3CRR and similar high luminosity radio sources as probes of galaxy evolution was probably premature and, in hindsight, unwarranted. They most likely represent the extreme bright end of the luminosity function and, if analyzed with care, they can offer valuable insights into the behavior of the most massive galaxies (e.g., de Brueck et al. 2003).

The weaker radio sources are thought to provide a safer vehicle for galaxy evolution studies and 53W091 is a prime example. Willots et al. (2001) have identified counterparts for a number of 7C radio galaxies that have very red $R - K$ colors. The majority of these objects appear to be members of the evolved class of faint red galaxies that host moderately active nuclei.

5.2. X-Ray Emission

The Chandra Deep Fields reach source densities of $\sim 10^4 \text{ deg}^{-2}$ in the hard X-ray bands (Alexander et al. 2003, Brandt et al. 2001, Giacconi et al. 2001). This population contains a total flux density that approaches that of the unresolved background (e.g., Alexander et al. 2001, 2003; Giacconi et al. 2001; Rosati et al. 2002). The vast majority of the sources is identified with optical counterparts brighter than $R \sim 26$ (Barger et al. 2003, Giacconi et al. 2001). It was noted early that a fraction of the faint Chandra sources is identified with galaxies having very red $R - K$ or $I - K$ colors (e.g., Scodreggio & Silva 2000). From deep near-IR studies of the Chandra Deep Field North (CDFN) Alexander et al. (2002) and Barger et al. (2003) found that 15% of the $I - K > 4$, $K < 20$ population are detected in the hard X-ray bands. These objects have relatively flat X-ray spectra and appear to be weak AGN. The detection rate is relatively flat with apparent K magnitude. Alexander et al. (2002) found that 10% of the red population to $K < 22$ are detected in the hard band. There is some suggestion that the X-ray fraction is higher for the reddest objects (e.g., $I - K > 5$; Alexander et al. 2002) but the numbers here are small. A comparable, although probably somewhat smaller, fraction of the red population is also detected at soft X-ray energies. These objects have spectral shapes and luminosities that are consistent with less energetic processes than the hard sources and are likely associated with star formation and normal hot gaseous halos. It is worth noting that EROs constitute only about 2% of the total X-ray source population.

Alexander et al. (2002) stacked images of a large number of red galaxies that were not detected directly in the 2 megasecond catalog and reported a high confidence level detection at a flux level consistent with typical X-ray emission from present-day elliptical galaxies. Brusa et al. (2002) carried out a similar analysis of the Chandra Deep Field South (CDFS), focusing on EROs with redshifts and spectroscopic classifications. They stacked Chandra images of $R - K > 5$ emission-line galaxies and found a significant detection implying an average $L_x \sim 8 \times 10^{40} \text{ ergs s}^{-1}$, whereas they did not detect a signal from a similar stack of

the objects with spectra dominated by old stars. Brusa et al. (2002) concluded that the hard X-ray emission traced star formation and inferred star-formation rates of $5\text{--}44 M_{\odot} \text{ yr}^{-1}$ from their stacked detection.

XMM-Newton observations have also revealed X-ray emission associated with a number of EROs (Stevens et al. 2003). These also have spectral shapes primarily consistent with an AGN origin, although some appear to be normal X-ray halos associated with a massive ellipticals. Only a small fraction ($\sim 5\%$) of EROs in the Lockman Hole field are detected by *XMM-Newton*, consistent with the Chandra results.

The X-ray results provide a unique window on the nature of the red galaxy population. The basic result appears to be that roughly 10% of the red galaxies contain actively accreting AGN at the level required to produce $L_x \sim 10^{42\text{--}43} \text{ ergs s}^{-1}$. At present, only about 1% of the massive elliptical galaxies contain luminous AGN, although dynamical studies suggest that essentially all elliptical and bulge-dominated systems contain massive black holes (Ferrarese & Merritt 2000, Gebhardt et al. 2000). The X-ray-detected ERO population in the Chandra Deep Fields have luminosities in the $0.1\text{--}2 \times 10^{43}$ range. The typical elliptical galaxy today has a nuclear X-ray luminosity that is two or more orders of magnitude fainter (e.g., Colbert & Mushotzky 1999), the fraction of present-day giant ellipticals with X-ray luminosities $> 10^{42}$ is quite small. Thus it appears that the X-ray results show that the rise in AGN activity to higher redshifts seen in quasars, radio galaxies, and other classes of AGNs extends to otherwise quiescent elliptical galaxies.

5.3. Morphologies

In principle, high spatial resolution imaging could cleanly settle the issue of what fraction of the red galaxies are passively evolving early-types and which are obscured star-forming galaxies. Imaging studies with the *Hubble Space Telescope* (*HST*) initially gave rather conflicting results, although some degree of consensus appears to be emerging in recent months. Treu & Stiavelli (1999) identified a sample of red galaxies from NICMOS images to be candidate $z > 1$ E and S0 galaxies. Stiavelli & Treu (2001) reported that most (60%) of the red objects had morphologies consistent with E/S0 *Hubble* types. Roughly 20% of the objects were classified as disk galaxies, primarily edge-on systems. A small minority of the red galaxies ($\sim 15\%$) appear to have irregular morphologies. This classification exercise was performed at rest-frame wavelengths well longward of 4000 \AA and thus should be a fair comparison with present-day morphological classifications.

Moriondo, Cimatti & Daddi (2000) examined the morphologies of red $R - K$ -selected galaxies in archival *HST* WFPC2, and NICMOS images. Moriondo et al. (2000) found a result quite similar to the Stiavelli & Treu distribution of morphologies, roughly 50–85% appearing to be early types, whereas the remainder are primarily disks with a small contribution from irregular types. The Moriondo et al. (2000) sample is fairly heterogeneous and does not constitute a complete

sample. Of particular interest is the 30% of the originally selected sample that had insufficient signal-to-noise ratios in the *HST* images to allow classification. These marginally or nondetected objects have lower surface brightness than the sample that was analyzed. Thus the fraction of objects with E/S0 morphologies in their parent sample could be as low as 50% if all of the faint galaxies have disk or Irr morphologies [hence the 50–85% range quoted in Moriondo et al. (2000)]. The median $I - K$ color appears to be correlated with morphological class, although the correlation is weak. The median color for their Irr class is $I - K = 5.5$, quite red indeed, whereas the E/S0 types have a median color of $I - K \sim 4.4$, quite near their nominal $I - K > 4$ threshold for inclusion into the sample.

P.J. McCarthy et al. (unpublished manuscript) has examined the morphologies of ~ 200 $I - K$ selected galaxies to $K < 20.8$ in the images from the Great Observatories Origins Deep Survey (GOODS) region of the CDFS. They found that the fraction of disks varies with color, but is nonnegligible in all of the color/magnitude subsamples. In the $4.0 < I - K < 4.5$ subsample, compact or early-type galaxies dominate, with disks contributing only 15–20%. Redder color selections (e.g., $4.5 < I - K < 5.0$ and $5.0 < I - K < 5.5$) yield higher fractions of disks and irregular and low-surface brightness, and thus difficult to classify, systems. The reddest color bins have disk fractions that are $\sim 50\%$.

Yan & Thompson (2003) carried out a program similar to those of Moriondo et al. (2000) and Stiavelli & Treu (2001), but rather than locating *HST* images of previously known red galaxies, they imaged several of the deepest *HST* pointings in the K -band from the ground. Yan & Thompson (2003) report nearly the opposite result from Stiavelli & True (2001) and Moriondo et al. (2000), finding that 60% of their red sample are disk systems, with roughly 30% elliptical/S0s and the remainder having irregular morphologies. There is no doubt from the *HST* images shown in Yan & Thompson (2003) that disks are ubiquitous in their red sample. There appears to be a preponderance of edge-on disks, and this suggests both large reddening as well as large bulge-to-disk contributions in these systems in the K -band.

Gilbank et al. (2004) used *HST* images from the Medium Deep Survey (Griffiths et al. 1994) in conjunction with ground-based K imaging to carry out a morphological analysis in the same spirit as the Yan & Thompson (2003) effort. They found that clear E/S0 galaxies and disks contributed in roughly equal numbers (30% of the sample each) and that objects with Irr morphologies contributed only 15% of the total. The remaining 15% were not classifiable. Gilbank et al. (2004) noted that a fraction of Irr galaxies appear to increase with redder colors ($I - K > 5$) and that the median color became redder at faint magnitudes ($K > 19.5$, see Section 4). Cimatti et al. (2004) analyzed the GOODS CDFS advanced camera for surveys (ACS) images in conjunction with a moderately complete (65%) redshift survey. They found results very similar to those reported by Gilbank et al. (2004), namely $\sim 1/3$ E/S0, $1/3$ disks, 15% Irr, and a small fraction of unclassifiable objects. Cimatti et al. (2004) noted that there was reasonable agreement between the morphological classification and the location in the two-color $R - K$ versus $J - K$

diagnostic of Pozzetti & Mannucci (2000). Both the studies by Cimatti et al. (2004) and Gilbank et al. (2004) found that there are objects with clear disk morphologies that are clearly in the passive evolution region of the two-color diagram (see below).

Recently the GOODS team carried out a detailed study of faint red galaxy morphologies from the deep ACS images in the CDFS (Moustakas et al. 2004). They found results similar in many respects to Yan & Thompson (2003), Gilbank et al. (2004) and Cimatti et al. (2004). Moustakas et al. (2004) reported E/S0 and disk fractions that are comparable at $\sim 30\text{--}40\%$ of the total. The remaining $20\text{--}30\%$ are found to be a mix of Irr, “chain galaxies” (Cowie et al. 1995), and objects too faint to classify. Moustakas et al. (2004) examined the spectral energy distributions of different morphological classes in detail and found that there is very little to distinguish between the spectral shapes of galaxies with disk and elliptical morphologies. This casts doubt on the simple two-color approach to separating the populations and appears to be in conflict with the results from Cimatti et al. (2004), Wehner et al. (2002), and Smail et al. (2002).

Reconciling these results is probably not as challenging as it first appeared. The samples obtained by Stiavelli & Treu (2001), Cimatti et al. (2004), and Moustakas et al. (2004) are on average fainter than the sample obtained by Yan & Thompson (2003). The Yan & Thompson (2003) sample, on the other hand, makes use of the deepest pre-ACS *HST* images and thus should give the most sensitive probe for low surface-brightness structures. The brighter ($K \sim 18$) samples may be expected to select on average a slightly lower redshift and more luminous sample than the fainter K -selected samples.

The GOODS/ACS images appear to support this as the brighter red objects do show a higher fraction of late-type morphologies (Moustakas et al. 2004). The steep luminosity function and narrow intrinsic color range of old ellipticals sharply cuts their redshift distribution for an $I - K > 4$ color cut and thus also sharply truncates their contribution to the counts at bright magnitudes. Late-type galaxies are likely to have a wider range of both intrinsic colors and greater sensitivity to inclination and variable reddening. Thus their broad color spread allows them to pass stringent color cuts at lower redshifts and they can compete with, or even dominate the contribution of early-types to the counts at magnitudes that correspond to K^* and brighter at $z \sim 1$. The current results suggest that passive ellipticals dominate at $K \sim 19\text{--}20$, disks contribute heavily to the counts at $K < 19$, and starbursts and Irr systems make an increasing contribution at faint ($K > 20$) magnitudes and redder colors. One wonders, however, if the high E/S0 fraction reported by Stiavelli & Treu (2001) might be strongly connected with their classification based on F160W images. Whereas the GOODS/ACS F814W and F980LP filters sample rest wavelengths near or just beyond the 4000 \AA break, they will still have significant contributions from current star formation, whereas the F160W images used by Stiavelli & Treu (2001) sample the 8000 \AA rest-frame spectrum and thus should give a clear sampling of the population that produces the red $I - K$ colors.

5.4. Photometric and Spectroscopic Discrimination

One might expect that photometric indices alone can distinguish between evolved and heavily reddened systems. The demonstration by Graham & Dey (1996) that the spectral energy distribution of HR10 is better fit by a reddened Sb spectral shape than an SED appropriate to an evolved system suggested that photometry alone might reveal similar systems. The primary discriminant lies in the shape of the spectrum near 4000 Å. Galaxies with ages of ~ 1 Gyr or more have spectral shapes that become flatter in the 4000–5000 Å range, and have a steep drop shortward of 4000 Å. Younger populations with sufficient reddening (and redshift) to achieve very red $R - K$ colors will have steeper slopes longward of 4000 Å, but may have UV slopes similar to those of old populations. The inflection in the evolved populations near 4000 Å is the basis of the two-color approach to distinguishing old populations from reddened starbursts developed by Pozzetti & Mannucci (2000). These authors showed that the two populations can be separated on this basis in a $J - H$ versus $H - K$ two-color diagram and they demonstrate that prototypes of each class behave as expected in this diagram. In practice the required photometric precision is often difficult to obtain. In figure 4 of Pozzetti & Mannucci (2000) one can see that many of the prototypes lie within 0.1 magnitude of the dividing line. Photometric accuracy at this level is often difficult to achieve, as Martini (2001) showed. In his sample, the majority of the objects are within one sigma of the discriminating line between starburst and ellipticals. Figure 5 in Smail et al. (2002) shows that several of their radio-detected red galaxies lie on the evolved-galaxy side (bluer in $J - K$) of the nominal dividing line, but the discrepancy is not large. Wehner et al. (2002) plot a similar diagram, but this one is based on $I - J$ versus $J - K$. They found that there is a significantly higher 850 μm flux density in the objects on the starburst region of the $I - J$ versus $J - K$ diagram. Pierini et al. (2004) and Bergstrom & Wiklind (2004) have examined the separation of the two populations in color space in some detail. Pierini et al. (2004) considered the case of galaxies that form in short bursts in the $1 < z < 2$ interval as well as old and multiple-burst populations in the same redshift interval, and concluded that in some cases very young objects can overlap with evolved populations in the two-color diagrams. Pierini et al. (2004) also concluded that the viability of the originally proposed $I - J$ versus $J - K$ diagram is not strongly dependent on the geometry of the dust and the degree of mixing between gas and stars.

Bergstrom & Wiklind (2004) suggested that a cleaner separation can be made in the $R - H$ versus $H - K$ two-color diagram, provided that the redshifts are below 1.4. Cimatti et al. (2003c) have examined the $R - K$ versus $J - K$ diagram with a sample that has both *HST* morphologies and spectral classifications from the K20 (Cimatti et al. 2002c) survey. Figure 6 shows the two-color diagram from Cimatti et al. (2003c). Three of the four star-forming galaxies with Irr morphologies lie to the right of the dividing line and the nine galaxies with old populations and compact morphologies lie to the left. Disk galaxies, however, are found on both sides the dividing line.

Thus it appears that these simple two-color diagrams have genuine utility in separating populations. To date, effort towards this approach has been focused on verifying the method. The difficulty in obtaining the requisite precision photometry for large samples does limit the applicability of this approach to the problem of separating young and old red systems. Observations at other wavelengths (e.g., the far-IR through radio) will ultimately prove more effective for statistical separations of the two populations.

Deep spectroscopic observations offer more information than broadband colors, but usually over a narrow range of wavelengths and primarily for brighter objects. Clear signatures of $A - K$ stars provide unambiguous evidence of truncated star formation and turn-off ages in the range of a few times 10^8 yrs to a few Gyr. Thus one can, in principle, discriminate between purely passive systems and objects that are dominated by on-going star formation that is partly obscured. The two prototypes in this respect are 53W091, the weak radio source that is identified with a >1 Gyr-old passive system, and HR10, the prototypical starburst ERO. Several deep spectroscopic studies of substantial samples of EROs have been completed recently. The K20 survey is the most advanced of these (e.g., Cimatti et al. 2002b). Whereas the median redshift of the K20 sample is below the relevant redshift of the ERO population, the sample is large enough that it reaches into the $z > 1$ range with significant numbers. The Gemini Deep Deep Survey (GDDS) (Abraham et al. 2004) targeted the $1 < z < 2$ range for K -selected samples and contains a fair number of $I - K > 4$ objects.

Cimatti et al. (2000) reported near-IR spectroscopic observations of a sample of EROs that shed some light on the nature of the bright near-IR light. They detected no strong breaks or emission lines, but they derived spectrophotometry that supplements the broadband photometry and is consistent with an evolved origin for the spectral shapes in the bulk of their sample. L. Yan & P.J. McCarthy (unpublished data) carried out a similar program (also with the *ISAAC* near-IR spectrometer on the VLT) for their NICMOS selected EROs and, again, detected no strong features in their J , H and K -Band spectra. Whereas HR10 first revealed its nature through near-IR spectroscopy (Graham & Dey 1996), few others have yielded to spectroscopy in the near-IR windows (but see Frayer et al. 2003). Recently, Saracco et al. (2002) have begun a low-resolution near-IR spectroscopic program using the NICS-Amici spectrometer that has yielded accurate spectral shapes for a number of bright EROs selected from the Munich Cluster Survey (MUNICS). This program targets bright objects $K' < 18.5$ and should sample the bright end of the red galaxy luminosity function. Given the results of the morphological studies this bright sample is likely to contain a fair number of luminous disk galaxies as well as massive ellipticals and should be particularly interesting.

Spectroscopy in the visible remains the most powerful approach to understanding the stellar content of the red galaxies. The advantages offered by multiplexing, low detector noise, wide wavelength range, and access to the rest-frame UV resonance lines outweigh the disadvantages of observing the objects in the region of the spectrum in which they are faintest. Cimatti et al. (2002a) produced high SNR

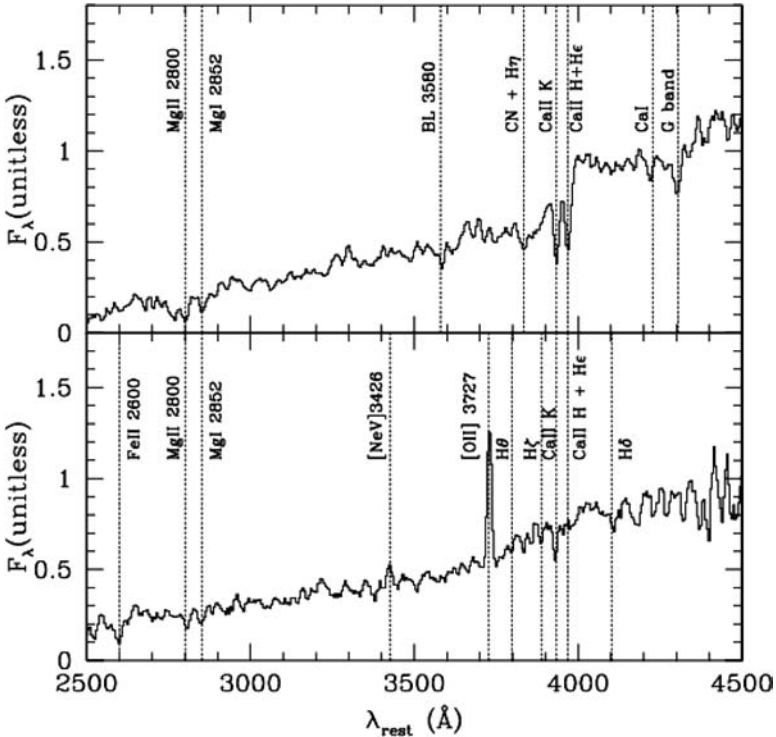


Figure 7 Composite spectra of passively evolving and actively star-forming red galaxies from the K20 sample by Cimatti et al. (2002a). Their composite old ERO spectrum (*upper panel*) and composite spectrum of objects identified as star-forming red galaxies (*lower panel*) are shown.

composite spectra representative of evolved red galaxies and reddened starbursts from the K20 survey, as shown in Figure 7. For $z < 1.3$ the evolved systems in the upper panel of Figure 7 can be recognized from their strong CaII *H* and *K* absorption and 4000-Å break features, while the starburst and post-starburst galaxies (lower panel of Figure 7) have strong Balmer absorption and often have significant [OII]3727 emission. Cimatti et al. (2002a) found equal numbers of pure absorption-line spectra and emission-line objects in their sample. From this they concluded that roughly 50% of their $R - K$ selected samples were reddened starbursts.

Yan, Thompson & Soifer (2004) obtained spectra of a significant sample of $I - K$ -selected red galaxies; a subsample of the galaxies for which they obtained deep *HST* imaging. Yan et al. (2004) reported that $\sim 85\%$ of the objects have absorption lines from old stars and that 50% of the sample showed pure absorption-line spectra. Half of the objects have emission lines in their spectra, in agreement with the K20 results by Cimatti et al. (2002a). Only 10–15% of the sample by Yan et al. (2004) appeared to have HR10-like spectra; strong emission lines and

steep continua. Yan et al. (2004) concluded that the majority of the light from the sample as a whole comes from evolved stars rather than an obscured population of massive stars, but they were unable to quantify this precisely.

The GDDS was built around some of the deepest spectroscopic observations to date. Abraham et al. (2004) presented the full catalog of 308 spectra of faint galaxies, some 43 of which are in the faint red galaxy class (e.g., $I - K > 4$, $K < 20.8$). The K20 samples and those by Yan et al. (2004) have yielded few spectra of evolved objects at $z > 1.3$. Abraham et al. and McCarthy et al. (2004) have shown that very long exposures can yield spectral features (MgI, MgII, FeII) in evolved red galaxies in the range of $1.3 < z < 2$, much in the same way as Dunlop et al. and Spinrad et al. (1997) did for 53W091. Abraham et al. (2004) classified their objects as being either young population-dominated, a mix of populations, or largely evolved populations. McCarthy et al. (2004) reported that roughly half of the GDDS $I - K > 4$ sample has spectra that are dominated by old stellar population. The remaining 50% are a mix of intermediate age and composite population systems.

Photometric, morphological, and submillimeter studies suggest that the starburst population becomes increasingly important at fainter magnitudes (e.g., $K > 20$) and redder colors (e.g., $I - K > 5$). This segment of the red population is poorly represented in the spectroscopic samples for obvious reasons (e.g., $K > 20$, $I - K > 5$, implies $I > 25$!). Thus to date the large spectroscopic samples address only the less extreme range of the population and thus are probably weighted more towards the passively evolving component of the ERO class. Whereas it can be argued that spectroscopy in the visible remains the most powerful approach, it suffers from the serious disadvantage of not sampling the red light on which the object selection and classifications are based. This can be detrimental in more ways than one. Massive ellipticals whose stellar-mass and K -band light is dominated by an early episode of star formation may have small amounts of ongoing, perhaps merger-induced, star formation that will dominate the rest-frame UV and thus lead to an erroneous classification of the object as primarily a starburst. Conversely, galaxies that are red owing to extinction are likely to be most heavily extinguished in the rest-frame UV. Patchy extinction will allow some objects, and perhaps the majority, to be recognized as star-forming systems, but extinction will render some impossible to detect spectroscopically in the visible (see e.g., Smail et al. 1999). Thus, samples that impose both a K -Band limit and an R - or I -band magnitude cutoff can be significantly incomplete. This applies to all of the samples discussed in the literature to date.

6. SPATIAL EVOLUTION

6.1. Redshift Distributions and Space Densities

The redshift distribution of early-type galaxies at high redshift provide a strong test of competing models of massive galaxy formation. The difficulties inherent

in separating the various contributors to color-selected samples can be overcome, to some degree, in spectroscopic samples and, in principle, the passively evolving population alone can be compared with the models. Complete K -selected samples suffer less from the impact of the reddened starbursts than the color-selected samples. The redshift surveys that reach $K \sim 19\text{--}21$ are best suited to this test (e.g., Abraham et al. 2004, Cimatti et al. 2002b, Cohen et al. 2000, Songaila et al. 1994).

Cimatti et al. (2002b) showed that the redshift distribution of the K20 sample is in good agreement with the pure luminosity evolution models by Pozzetti et al. (1996, 1998) and in serious disagreement with the semianalytic hierarchical-merging models. The K20 redshift distribution is a combination of spectroscopic and photometric redshifts. While there is disagreement with the semianalytic models at low redshift (they predict more faint galaxies than observed), the difference is modest compared to the discrepancy at the high redshift end. The semianalytics predict approximately four times too few galaxies at $z > 1.5$ compared to the data. Most of the redshifts in this interval are photometric; thus there is some uncertainty in the details of the comparison. Firth et al. (2001) used photometric redshifts for a large sample of H -band-selected galaxies and found three times more $z > 1$ red galaxies than predicted by the semianalytic models. Both samples are heavily dependent on photometric redshifts at $z > 1.3$ (the sample by Firth et al. 2001 is all photometric), yet it seems quite likely that the basic $N(z)$ is not seriously in error and that there is a tail to high redshifts that is in conflict with the semianalytic models. Figure 8 shows the $N(z)$ from the K20 sample and predicted redshift distributions for Hierarchical Merger Model (HMM) curves from Cimatti et al. (2002b). This shows clearly that there is an overabundance of $z > 1.5$ galaxies compared to the HMM models. More recent models (e.g., Somerville et al. 2004) do a far better job at matching the $N(z)$ for complete K -selected samples. They still have difficulty matching both the color and redshift distributions, predicting too few red galaxies at high redshift.

Stanford et al. (2004) have taken a somewhat different approach, using a morphologically selected sample of early types from the HDF-N. Again, using a mix of spectroscopic and photometric redshifts, they examine the $N(z)$ for early types and found better agreement with the hierarchical models than with the PLE model. The small field-of-view of the HDF-N does make their conclusion subject to the impact of large-scale structure and sample variance. Barger et al. (1999) reached a similar conclusion based on the surface density of $I - K > 4$ objects. Their sample, while covering a larger area than the NICMOS HDF-N data, was centered on the same region of sky, and thus is susceptible to the same sample variance. Similarly, the Franceschini et al. (1998) study of early-type galaxies in the HDF-N does not provide a truly independent estimate of the space density of red ellipticals at $z \sim 1$.

6.2. Clustering of Red Galaxies

One of the more remarkable aspects of the red galaxies is their high degree of spatial clustering. Daddi et al. (2000) and McCarthy et al. (2001) detected strong angular

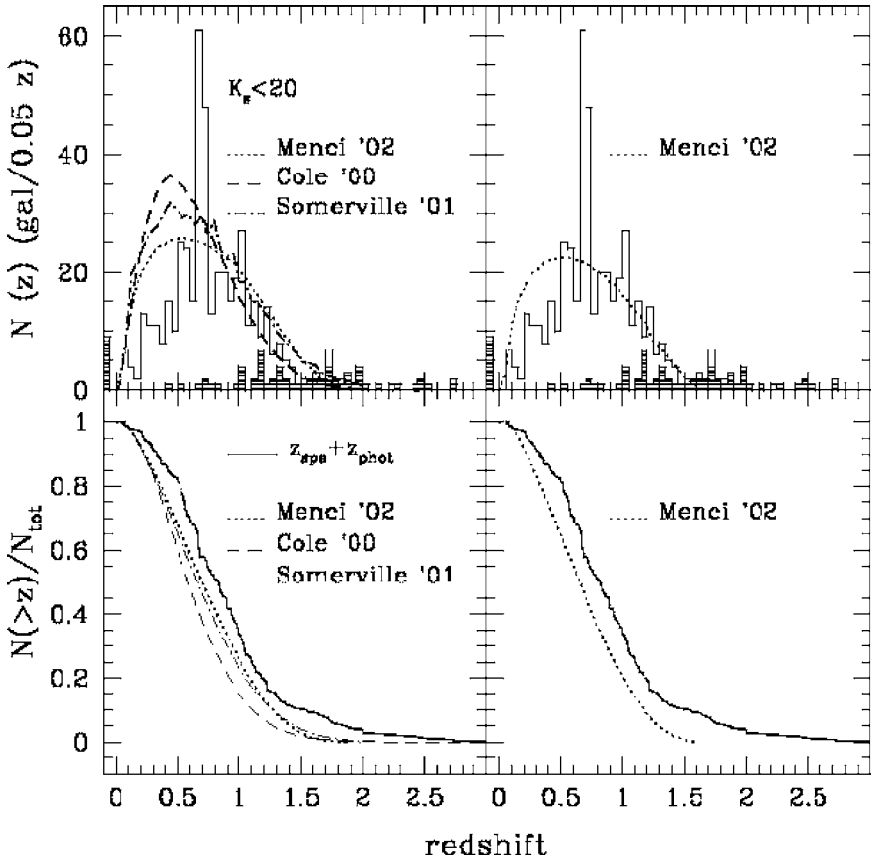


Figure 8 The redshift distribution from the K20 sample compared with hierarchical merging models (from Cimatti et al. 2002b): observed differential $N(z)$ from the K20 survey, including both spectroscopic and photometric redshifts compared with the HMM models of Menci et al. (2002), Cole et al. (2000), and Somerville et al. (2001) (*upper panels*); cumulative histograms (*lower panel*); observed $N(z)$ (*solid line*); the models (*dashed lines*). At $z = 1.5$ there is a clear excess of galaxies compared with the HMM models. Comparisons with PLE models can also be found in Cimatti et al. (2002b).

clustering in moderate area samples of red galaxies, defined by $R - K > 5.5$ in Daddi et al. (2000) and $I - H > 3$ in McCarthy et al. (2001). The amplitude of the angular correlation function in the red samples is $\sim 12\text{--}15''$, approximately ten times that of the full K -selected field sample ($\sim 1.5''$). The amplitude of the clustering increases both with redder colors and at brighter apparent magnitudes. Angular clustering strengths as large as those seen in the bright red population ($\theta_0 \sim 30''$) are extremely rare and point to either a very high degree of three-dimensional clustering or a narrow redshift slice, or both. The high degree of

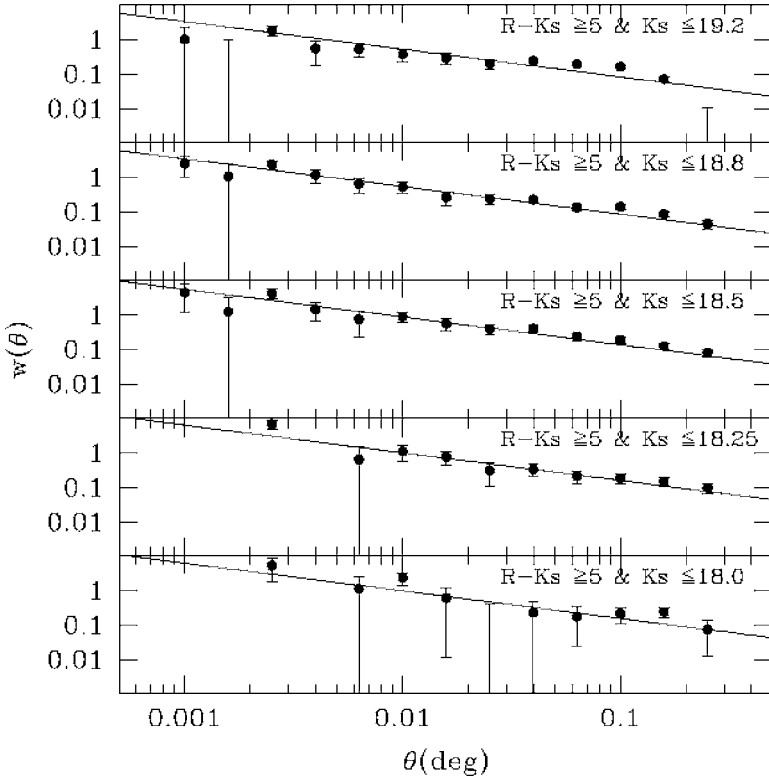


Figure 10 Angular correlation functions for various color and magnitude cuts from Daddi et al. (2000). The strong clustering of the red objects and the increasing amplitude at bright magnitudes is quantified by these determinations of $w(\theta)$.

clustering is clearly visible in maps of the red galaxies. Figure 9 shows a map of a $26' \times 26'$ of sky with objects color coded on the basis of their $I - K$ colors. The red galaxies are clearly strongly clustered. The angular correlation function quantifies the degree of clustering and Figure 10 shows an example $w(\theta)$ from Daddi et al. (2000).

The three-dimensional clustering length can be recovered from the angular clustering given a redshift distribution for the parent sample via the Limber equation (Limber 1953, Peebles 1980). In simple terms, the strength of the angular clustering signal that arises from a given degree of spatial clustering depends on the thickness of the redshift shell and the distance to the shell. At redshifts near one, the derived value of r_0 depends only weakly on the median redshift, but it depends strongly on the width of the redshift shell. The strong angular clustering signal for the red galaxies reflects both a high degree of intrinsic clustering as well as the effectiveness of simple optical-to-IR color selection in isolating a narrow shell in redshift.

McCarthy et al. (2001) and Firth et al. (2001) used photometric redshifts to estimate the redshift distribution of their $I - H$ and $R - H$ selected samples. This led to a fairly narrow redshift range, $\langle z \rangle \sim 1.1$, $\sigma(z) \sim 0.15$ for a sample defined by $I - H > 3$, $H < 20.5$. Brighter samples have a somewhat smaller $\sigma(z)$, whereas redder samples have a slightly higher mean redshift. The photo- z derived redshift distributions lead to inferred comoving correlation lengths, r_0 , of $9 \sim 11h^{-1}\text{Mpc}$ ($h = H_0/100 \text{ km s}^{-1} \text{ Mpc}^{-1}$) in McCarthy et al. (2000) and $6h^{-1}\text{Mpc}$ in Firth et al. (2001). Daddi et al. (2001) used a pure luminosity evolution model to derive a redshift distribution for their $R - K > 5$, $K < 19.5$ sample. The PLE models have a tail to higher redshifts than the $N(z)$ derived from the photometric redshifts and thus Daddi et al. (2001) derive a larger clustering scale, finding $r_0 \sim 12h^{-1}\text{Mpc}$. The difference between the two approaches is not all that large given the substantial uncertainties in each measurement and both approaches imply large correlation lengths. Spectroscopically determined redshift distributions (e.g., Yan et al. 2004) show that the basic inference from either the photo- z 's or PLE models is correct, namely that the characteristic redshift is ~ 1.1 . The Yan et al. (2004) $N(z)$ favors the lower r_0 , but it is likely to be incomplete at $z > 1.5$. The high redshift tail predicted by the PLE models are hard to verify as most samples become incomplete at $z > 1.5$, although the GDDS is probably least effected. The $R - K$, $I - K$, or $I - H$ selected samples are not likely to be pure samples of passively evolving systems, and thus there will be interlopers compared to the estimates of $N(z)$ based on either simple evolution models or photo- z determinations. As seen clearly from the submillimeter and X-ray studies there is more than one class of red galaxy, and there are reasons to believe that their redshift distributions are not the same and that the starburst population extends to higher redshifts and should have a smaller correlation angle. Indeed, Daddi et al. (2001) found that the angular clustering strength of red galaxies with spectral features indicative of ongoing star formation is much weaker than that of passively evolving populations, and they infer $r_0 < 2.5h^{-1}\text{Mpc}$ for the starburst ERO population.

The clustering amplitude of the red galaxies is larger than that of the other well-studied galaxy populations at high redshifts. The Lyman-Break galaxies (LBGs) have a clustering strength of $r_0 \sim 4h^{-1} \text{ Mpc}$ (Giavalisco & Dickinson 2001, Giavalisco et al. 1998). The most luminous LBGs reach clustering amplitudes of $r_0 \sim 6h^{-1}\text{Mpc}$, closer to the lower end of the ERO r_0 determinations. Clustering strengths for large samples of LBGs and Lyman alpha emitters have been determined from the Subaru Deep Survey (SDS) using techniques similar to those applied to the EROs (Ouchi et al. 2004). The reddest subset of the LBGs from the SDS appears to have a clustering strength ($r_0 \sim 8h^{-1}\text{Mpc}$), that is not dissimilar to that of the EROs.

Brown et al. (2003) have used the larger NOAO Deep Wide Survey (Jannuzi et al. 2002) sample to determine clustering strengths using the $w(\theta)$ approach. They found that the most luminous red (in $R - I$) galaxies at $z \sim 0.8\text{--}10$ have $r_0 \sim 6h^{-1}\text{Mpc}$ and thus appear to be in conflict with the ERO clustering measurements. Different approaches to estimating $n(z)$ are part of the difference, but it is also

quite likely that $R - I$ selections do not recover the same population as the $R - K$ or $I - K$ samples. Brown et al. (2003) argued that the PLE-based determinations of r_0 for the $z \sim 1$ EROs are overestimates.

Locally, the only galaxies that have correlation lengths as large as $10h - 11$ Mpc are morphologically selected giant ellipticals. Guzzo et al. (1997) derive $r_0 = 11.3 \pm 1.3h^{-1}$ Mpc for early-type galaxies with $M_B < -19.5 + 5 \log(h)$ from the Pisces-Perseus supercluster survey, while Willmer et al. (1998) derive a significantly smaller value from the SSRS2 redshift survey. Fainter samples of galaxies with spectral shapes indicative of ellipticals have been analyzed as part of the Sloan Digital Sky Survey (SDSS). These samples yield smaller correlation lengths; Budavari et al. (2003) measure $r_0 = 6.6 \pm 0.17h^{-1}$ from photometric redshifts, while Zehavi et al. (2002) derive $r_0 = 7.4h^{-1}$ Mpc for galaxies brighter than $M_\star - 1.5$. Daddi et al. (2002) and Rottgering et al. (2004) note that locally radio galaxies have large clustering lengths (Peakcock & Nicholson 1991) and that the high degree of correlation between elliptical host and luminous radio sources provides an interesting comparison point for the distant samples. Indeed, the luminous radio galaxies probe an even rarer and more massive subset of the red galaxies at intermediate and high redshifts and so their strong clustering lends some credence to the large r_0 values inferred for the bright ERO populations.

Theoretical models predict that the clustering amplitude of the evolved galaxies should be nearly constant with redshift (Kauffmann et al. 1999). Figure 7 of Kauffmann et al. (1999) shows that the expected clustering amplitude for early-type systems is roughly flat at $r_0 \sim 7h^{-1}$ to $z \sim 2$, and is approximately three times that of the blue/star-forming populations. Qualitatively, the behavior of the Lyman-Break Galaxy (LBG) agrees with the predictions in Kauffmann et al. (1999), although normalization appropriate to the ERO clustering $z = 0$ is somewhat uncertain, as it is with the LBGs as well (Giavalisco et al. 1998).

7. FORMATION, AGES, AND SPECTRAL EVOLUTION

7.1. The Evolving Luminosity Function of Early-Type and Red Galaxies

Luminosity functions are the next step in understanding the red galaxies beyond simple space densities. They not only give a detailed census of the galaxy population, but also provide a breakdown of the galaxies by luminosity. The ultimate goal, the mass function, is a fairly straightforward step from the luminosity function. The K -Band luminosity function is of particular interest as the derivation of either the comoving mass density or the full mass function are most securely carried out from observations that sample rest-frame wavelengths well beyond 4000 \AA . Kauffmann & Charlot (1998) show that the K -Band LF is a sensitive discriminator between the monolithic collapse, as in Eggen, Lynden-Bell & Sandage (1962) and its modern descendants (Sandage 1986, 1990), and the hierarchical formation models. The hierarchical and PLE models predict factors of three to five

differences in the space density of K -selected galaxies at $z = 1$. The models in Kauffmann & Charlot (1998) were based on a $q_0 = 0.5$, $\Lambda = 0$ cosmology. The currently favored concordance cosmology ($\Omega = 0.3$, $\Omega_\Lambda = 0.7$) yields smaller differences at $z \sim 1$ and pushes the critical proving ground to higher redshifts.

The seminal study of evolution in the field galaxy luminosity function came from the Canada-France-Hawaii redshift survey (Lilly et al. 1995a). Lilly et al. (1995b) showed that the red component of the galaxy population (defined by $V - I$ colors) has evolved little, if at all, since $z \sim 0.8$. Whereas the blue population exhibits a steep evolution in luminosity density, the red galaxy luminosity density shows less evolution than expected from simple passive evolution. Other studies focused on morphologically selected samples of early types at $z \sim 1$ reported mild evolution. Ellipticals in the *HST* MDS show 0.5–1 magnitude of brightening to $z \sim 1$ (Im et al. 1996). Ellis et al. (1996) examined the B -Band LF as a function of [OII] equivalent width. Even though the Ellis et al. (1995) sample was B -selected and not color-segregated they recognized that the bright [OII]-weak (i.e., inactive) component of the field galaxy population showed little or no evolution to $z \sim 0.75$. Galaxies selected by their absorption cross-section also exhibit little or no evolution in their K -Band LF to $z \sim 0.8$ (Steidel, Dickinson & Persson 1994). Thus there is fairly good agreement that red color-selected samples show little evolution in the K -Band LF to $z = 1$. Color selections that are too stringent can lead to apparent declines in the luminosity function, or space density, that are heavily influenced by passive color evolution. This may be behind the apparently flat behavior of the K -Band LF in some color-selected samples. Morphologically selected samples include a wider range of colors and show a degree of luminosity evolution in line with that expected from purely passive evolution and modest (e.g., $2 < z < 5$) formation redshifts (e.g., Lubin & Sandage 2001).

Wolf et al. (2003), Chen et al. (2003), and Bell et al. (2003b) have used photometric redshifts to derive luminosity functions to $z \sim 1.3$. A number of issues come into play with photo- z treatments of the LF, the most significant being the large redshift uncertainties and the biases that come with them. Chen et al. (2003) treated the redshift uncertainties explicitly and found no apparent evolution in the LF of galaxies with spectral shapes matched to E/S0 & Sa templates, nearly equivalent to a color cut in $I - H$ or $R - H$. The lack of evolution in the rest-frame R -band luminosity density implies a declining mass density. Chen et al. (2003) estimate that this amounts to a factor of ~ 2 or less at $z = 1.2$.

Wolf et al. (2003) used the 17 medium-band filter photometry of the COMBO-17 survey (Bell et al. 2003a) to derive luminosity functions for a range of spectral types over the $0.2 < z < 1.2$ interval. The large number of intermediate-band filters used in the COMBO-17 survey yields very precise photometric redshifts and its substantial survey area (0.78 square degree) provides not only large sample sizes, but also mitigates against the impact of large scale structure. Wolfe et al. (2003) reported a dramatic decline in the number and luminosity density of early-type galaxies from $z \sim 1$ to the present. The Wolf et al. spectral classifications were based on a set of nonevolving templates. These are not well suited to early spectral

types and particularly at visible wavelengths, where passive evolution results in significant color evolution. As shown in Figures 1, 2, and 11, a nonevolving elliptical SED (e.g., Coleman, Wu & Weedman) defines the red envelope rather than a median spectral shape and hence will exclude a significant number of genuine early-type galaxies. The effect is larger for purely visible band photometry than that seen in the $I - K$ or $R - K$ planes.

Bell et al. (2004) also used the COMBO-17 photometric survey to derive evolving luminosity functions. In this analysis they separated the galaxy populations into blue and red components on the basis of an empirically determined color distribution. The red field population shows a color-magnitude trend similar to that seen in clusters, and this red sequence evolves as expected from passive evolution. Like Chen et al. (2003), Bell et al. (2004) found little evolution in the red galaxy LF, particularly at the bright end. The large decline in the number of red galaxies reported by Wolf et al. (2003) was found by Bell et al. (2004) to be heavily influenced by passive evolution in the colors of the earliest spectral types. A similar effect likely played a role in the strong evolution in early types derived from the Hawaii survey data set by Kauffmann, Charlot & White (1996) and in the conclusion by Zepf (1997) that there were no high redshift ellipticals in the HDF-N.

Pozzetti et al. (2003) used the K20 spectroscopic sample to derive J - and K -Band luminosity functions. They found only mild evolution in the K -Band LF to the highest redshifts, $\Delta M_K \sim -0.544$ at $z = 1$. This was ~ 0.5 mag less than the expectation from pure passive evolution, and implied that the space density of luminous early-type galaxies has declined by only $\sim 30\%$ since $z = 1$. This nearly constant density of luminous red galaxies is consistent with the crude estimate from galaxy counts in McCarthy et al. (2001) and Chen et al. (2002) and the $n(z)$ derived from the K20 survey by Cimatti et al. (2002b). Chen et al. (2004) recently applied a photometric redshift approach to the LF to derive rest-frame J - and K -Band LFs in the $1 < z < 2$ range from a sample of ~ 4000 galaxies. They found excellent agreement with the Pozzetti et al. (2003) $0.75 < z < 1.3$ LF in the region of overlap (the bright end). The photo- z derived LF extended ~ 2 magnitudes fainter than the K20 spectroscopic redshift, albeit with larger systematic uncertainties. Chen et al. (2004) LF showed approximately 0.5 mag of brightening at the bright end when compared to local determinations (e.g., Kochanek et al. 2001), again in agreement with Pozzetti et al. (2003). Glazebrook et al. (2004) used the GDDS spectroscopic survey to compute a K -Band LF at $1 < z < 1.5$ and also found good agreement with both the large photo- z -based determination and the K20 direct measurement.

There appears to be a consensus now that the luminosity function of red galaxies shows little apparent evolution to $z \sim 1.5$ and that this is in some disagreement with theoretical expectations based on hierarchical merging models. The discrepancy between theory and observation is laid out in Pozzetti et al. (2003). There is both an excess in the predicted number of sub- L_* galaxies at modest redshifts and a significant deficit in the expected number of luminous galaxies at high redshift. This is most dramatic at $z \sim 1.5$ where Pozzetti et al. (2003) found an

order-of-magnitude–more galaxies with $M_K < -26.5$ compared to either the Cole et al. (2000) or Menci et al. (2002) models. More recent refinements to the semianalytic models (Somerville et al. 2004) reduce this discrepancy considerably. Morphologically defined samples of ellipticals do not yet reach redshifts as high as the color-defined samples, but they show larger luminosity evolution, implying less mass accumulation since $z = 1$. This is likely the result of these samples being more complete as they contain both red and blue ellipticals. At the highest redshifts ($z > 1.5$) the red color-defined samples likely suffer from significant contamination from reddened late-type systems and thus the degree of mass and luminosity evolution at these redshifts is less certain.

7.2. The Color-Magnitude and Color-Color Relations

In Section 1 we introduced the color-magnitude diagram as a basic survey tool; it contains two of the keys aspects of the evolution of the constituent stellar populations, color (a proxy for age) and luminosity (age and mass). The key element, redshift, is folded into both axes and so critical information is lost. The CMD is useful, however, for examining large samples for which redshifts are not available and for getting a clear picture of the extremes of the populations for which redshifts are unlikely to be available.

Two-color diagrams were discussed above primarily as a tool to separate old and young galaxies in the presence of significant extinction. These diagrams can also be powerful probes of stellar content and evolution, particularly when used in combination with photometric and spectroscopic redshifts. Figure 11 shows the $V - I$ versus $I - K$ diagram from a 0.2 square degree area of the Las Campanas IR survey. The points are color coded by photometric redshifts and evolutionary tracks ranging from no evolution to constant star formation are overlaid. Moustakas et al. (1997) presented an early version of this diagram from their deep NIRC imaging survey.

There is a tendency in the literature to classify each of the red galaxies into one of two very different bins, either pure passively evolving systems or heavily obscured actively star-forming systems. There are good reasons to expect that the reality is not so cleanly divided into two extremes. Early forming and slowly evolving galaxies can undergo modest star-formation episodes (or even massive bursts) associated with merger events. These objects will depart from the purely passive colors in the rest-frame UV and may have strong emission lines and yet, if the burst strength is small, the K -Band light can be dominated by the old population. Composite objects might be expected to be more common at high redshift, particularly if the merger rate increases with look-back time. The two-color $V - I$ versus $I - K$ diagram suggests that the higher redshift red $I - K$ population has bluer rest-frame UV colors. In Figure 11 the objects with red $I - K$ and blue $V - I$ appear to be at higher redshifts than those that lie closer to the pure-passive line (red in both $I - K$ and $V - I$). Whereas young systems can masquerade as old galaxies in broadband colors, primarily old systems can appear to be young

in rest-frame UV emission line and continuum spectra. Thus the separation of the population into purely passive and active classes is blurred and may be artificial.

7.3. Ages and the Formation Epoch

Perhaps the most interesting issue in the study of the evolved red galaxy population concerns the assembly and star-formation histories of objects that evolve into present day elliptical galaxies. Elliptical galaxy and spiral bulge formation is usually couched in one of two simple conceptual frame works: monolithic collapse and hierarchical assembly via mergers. In the monolithic collapse model (Eggen, Lynden-Bell & Sandage 1962; Sandage 1986, 1990) early-type galaxies collapse and convert most of their gas into stars in a dynamical time. The chemical homogeneity, internal dynamics, and colors of present-day elliptical galaxies can be understood in an early collapse model that has a high degree of violent relaxation. The alternative view, hierarchical formation of large systems from the merging of smaller ones, also has its roots in attempts to understand the Milky Way halo (Searle & Zinn 1978). The recently discovered dynamical substructures in the Milky Way halo show that at some level the Searle-Zinn process is occurring today. In the hierarchical models elliptical galaxies, and indeed all massive galaxies, are formed from mergers of many subunits. In numerical models of merger histories the merger trees for massive elliptical progenitors can be quite complex and involve tens of merger events of various mass ratios. The semianalytic models (Cole et al. 2000, Somerville & Primack 1999) aim to reproduce the properties of real galaxies within a particular cosmological world model, and thus they provide a test bed for comparison between theory and observation. Empirical approaches to the question of the formation mode and epoch center on the evolution of colors, masses, space densities, and luminosity functions with redshift. Each offers a different way of getting at either the stellar content of galaxies or the number of “finished” systems per unit of comoving volume.

Colors alone are a crude tool and they are susceptible to degeneracies and reddening. Nevertheless, they provide a useful starting point from which to gauge the evolution of stellar populations. Figure 12 shows the observed $I - K$ colors of a sample of ~ 600 galaxies from the combined LCIR and GDDS sample, along with tracks for simple galaxy evolution models. Also included are the color of K^* galaxies from the cluster samples of Stanford et al. (1995, 1998) and Chapman, McCarthy, & Persson (2000), along with LBGs from the HDF-N (Papovich et al. 2001). The cluster points show the color of K^* at the cluster redshift. The tracks in Figure 12 show the trajectories of a nonevolving elliptical galaxy redshifted through the band-passes (dashed red line): two models with $z_f = 20$ and exponentially declining star formation with e-folding times of 1 Gyr and 2 Gyr (solid back lines), and four $\tau = 0.5$ Gyr models with $z_f = 2$ (cyan), 3 (blue), 5 (green), and 10 (red). The 0.5 Gyr exponential model with $z_f = 10$ forms a reasonable benchmark for a minimal evolution scenario. The K -selected field galaxies span the full range of available colors and track the red envelope defined by the minimal evolution model

fairly well. There are a few galaxies redder than the minimal evolution envelope at low redshift but they are a small minority. The red envelope in the field appears to follow that of the clusters, as shown by the agreement between the cluster color evolution (filled triangles in Figure 12) and the red extreme of the field galaxy colors as a function of redshift. Given that this locus is sensitive to both formation epoch and metal content, it suggests that the oldest populations in the field and in rich clusters are not dissimilar.

The colored tracks in Figure 12 correspond to rapidly evolving PEGASE2 models with formation redshifts ranging from two to ten. These tracks are meant to address the issue of evolutionary connections between the LBG and passive red populations. At face value the tracks suggest that formation redshifts of $z_f \sim 3-4$, appropriate to the LBG population, are challenged to reach the red colors of the passive population by $z \sim 2$. The high star-formation rates and large reddening of the SCUBA bright population and the $J-K$ selected galaxies (Franx et al. 2003) are better candidates for progenitors of the $z \sim 1.5$ red galaxies. Figure 12 lends strong support to the idea that the reddest galaxies trace an early-forming population. The rapidly evolving, or late forming, models do not reach the red envelope defined by either the field or cluster sequences. Formation redshifts significantly less than five are challenged by the colors of the reddest galaxies at $z \sim 2$.

Spectra contain more information regarding the age and stellar content than do broadband colors, although usually over a limited range of wavelengths. The deep Keck spectra of 53W091 (Dunlop et al. 1996, Spinrad et al. 1997) show the value of high quality spectra combined with multicolor photometry. The clear detection of F-star features in 53W091 led Dunlop et al. (1996), Spinrad et al. (1997), and Jimenez et al. (1999) to infer an age for this system of 3 Gyr or larger. This age was challenged by Bruzual & Magris (1997) and Yi et al. (2000). Bruzual & Magris (1997) argued that the spectral breaks used by Spinrad et al. (1997) to infer an age of 3 Gyr are less sensitive to the turn-off age than suspected as they contain significant contributions from the lower main sequence. Bruzual & Magris (1997) infer ages in the range from 1–2 Gyr. Yi et al. (2000) used the Yale models to fit both the spectrum and the full spectral energy distribution from the photometry and infer an age in the 1.4–1.8 Gyr range, consistent with the Bruzual & Magris (1997) result. Nolan et al. (2001) rebut the Yi et al. (2000) result and show that the Jimenez et al. (1999) models give best fitting ages of 3 Gyr. They also fit the radio galaxy 53W069 ($z = 1.43$) and derive best fitting ages of 5–6 Gyr for the Jimenez (1999) models, whereas the Yi et al. (2000) models give ages in the two to four Gyr range.

Spectroscopic studies of red galaxies from K -Band field surveys have revealed clear evidence of evolved stars in a significant fraction of the population (Cimatti et al. 2002a; Yan, Thompson, & Soifer 2004), but these are usually confined to $z < 1.3$ and so do not provide as much leverage on the formation redshift as does 53W091. The time interval between $z = 1.3$ and $z = 2$ is 1.4 Gyr in the concordance cosmology, so there is a considerable premium on obtained spectral diagnostics at the highest possible redshifts (McCarthy et al. 2004).

Figure 13 shows spectra of the prototypical old red galaxy 53W091, a composite of 5 $z > 1.6$ red galaxies from the GDDS and a spectral synthesis model with an age of 3 Gyr. Superposed on the GDDS $z > 1.6$ red composite is the composite luminous red galaxy from the Sloan Digital Sky Survey (Eisenstein et al. 2003).

8. MASS EVOLUTION

One of the key goals of galaxy evolution studies is to determine the evolution of the stellar content of galaxies. Colors and luminosities are observables that provide information on the ages and star-formation rates, but physical models of galaxy formation deal primarily with mass. Dynamical studies probe the evolution of total galaxian masses at high redshift and may offer the closest link to the growth of dark matter halos. Stellar masses, however, provide a key gauge of the process of galaxy building and provide a constraint on models of the evolution of the cosmic star-formation rate, the buildup of heavy elements and merger rates. Ultimately the global star-formation history (Madau et al. 1996) and the global stellar-mass-density evolution should paint a consistent history of galaxy formation and assembly.

The basic approach to determination of the stellar masses of galaxies is fairly straightforward. Spectral synthesis models are fit to energy distributions. Stellar mass-to-light ratios are then derived from the spectral synthesis models and the total luminosity at some fiducial wavelength is used to convert luminosity to mass. As we are only interested in the mass in stars we need not worry about dark matter. Stellar-mass estimates with uncertainties as low as $\pm 50\%$ are possible (e.g., Brinchmann & Ellis 2000, Kauffmann et al. 2003). Accurate mass-to-light ratios are clearly the key to this process, and it is encouraging that fundamental plane analyses give M/L values that are in reasonable accord with the spectral fitting approach (e.g., Jorgensen et al. 1999, van der Wel et al. 2004, van Dokum & Stanford 2003).

The Sloan Digital Sky Survey provides a local determination of the total stellar-mass density and a determination of the relative contribution of galaxies of different types to the present-day mass density. Most the stellar mass today appears to be in galaxies of modest mass ($5 \times 10^{10} M_{\odot}$; Kauffmann et al. 2003), and the mass appears to be roughly evenly divided between disks and spheroids (Schechter & Dressler 1987). Brinchmann & Ellis (2000) inferred a decline in the stellar-mass density in irregular systems accompanied by a rise in the mass density in elliptical galaxies since $z \sim 1$ from *HST* images of the CFRS sample. Brinchmann & Ellis (2000) infer a fairly constant mass density in disk galaxies for the last half of the *Hubble* time. The mass evolution of the early-type galaxy population is of particular interest as it is likely to be more closely related to early merging of stellar systems rather than to the steady conversion of gas into stars as is the case for quiescent disk galaxies. At redshifts in excess of unity the difference between

the stellar masses of elliptical galaxy progenitors in the hierarchical and monolithic collapse models becomes substantial and at some sufficiently large redshift there should be few or no massive red galaxies in the hierarchical models.

The Bell et al. (2003b) COMBO-17 analysis of the red sequence yields a modest evolution in M/L (about a factor of 2) since $z \sim 1$. From this Bell et al. (2003b) infer an increase in the total stellar mass in red galaxies since $z \sim 1$ by a similar amount. Franx et al. (2003) used the Faint IR Extragalactic Survey (FIRES) to carry out a census of red galaxies at $2 < z < 3$. Rudnick et al. (2003) measured the mass evolution in this sample and concluded that there has been a factor of ~ 3 growth in the stellar mass of galaxies since $z \sim 2.5$ and that roughly half of the stellar mass in galaxies at $z = 3$ is in galaxies redder than those in the Lyman-Break selected samples. Dickinson et al. (2003) have inferred a more dramatic increase in stellar-mass density since $z \sim 4$ from the *Hubble* Deep Field data. Shapley et al. (2001) determined that the LBGs at $z \sim 3$ contain only 20% of the present-day stellar-mass density, whereas Dickinson et al. (2003) found only 5% of the present density at $z \sim 5$.

The total stellar mass as a function of redshift is one of the critical pieces needed to understand galaxy formation. Of equal interest is the maximum stellar mass achieved by galaxies at any epoch. The high-mass objects probe the most overdense regions and, possibly, the earliest-forming systems. Hierarchical models predict both a decline in the total stellar-mass density to high redshift and a decline in the maximum mass observed in galaxies.

Daddi et al. (2004) identified a number of highly luminous galaxies at $z \sim 2$. These objects have K magnitudes of 18.7–20 and are thus quite luminous. Mass estimates range from 3×10^{10} – $5 \times 10^{11} M_{\odot}$. These objects are forming stars at very high rates (~ 200 – $500 M_{\odot} \text{ yr}^{-1}$) and Daddi et al. (2004) suggest that these are spheroids in the process of formation. Glazebrook et al. (2004) measured the masses of a representative sample of K -selected galaxies in the $1 < z < 2.5$ range from the GDDS sample. Glazebrook et al. (2004) found that the maximum mass evolved little between $0.5 < z < 2$ and is $\sim 3 \times 10^{11} M_{\odot}$ (also see Fontana et al. 2004). Unlike the GOODS/Daddi et al. (2004) sample, the GDDS/Glazebrook objects appear to be largely devoid of ongoing star formation, rather they appear to be passively evolving high-mass galaxies. Stanford et al. (2004) found similarly massive ($> 10^{11} M_{\odot}$) red galaxies with early-type morphologies in the HDF-N, although in small numbers. Figure 14 shows the derived masses of galaxies with $K < 20$ from the Glazebrook et al. (2004) GDDS sample and the Daddi et al. (2004) GOODS/K20 sample. One can easily see the essentially flat distribution of maximum mass with redshift over the full range from $0.5 < z < 2.5$. This is a remarkable plot as it suggests that the most massive galaxies were firmly in place at quite early times. The number of massive galaxies in the GOODS/K20 sample is far in excess of predictions of semianalytic models of galaxy formation. Daddi et al. (2004) estimate that their derived space density of galaxies with $M > 10^{11} M_{\odot}$ exceeds the Baugh et al. (2003) predictions by a factor of ~ 30 or greater. Similarly, Glazebrook et al. (2004) measured a space density of galaxies with $M > 10^{11} M_{\odot}$

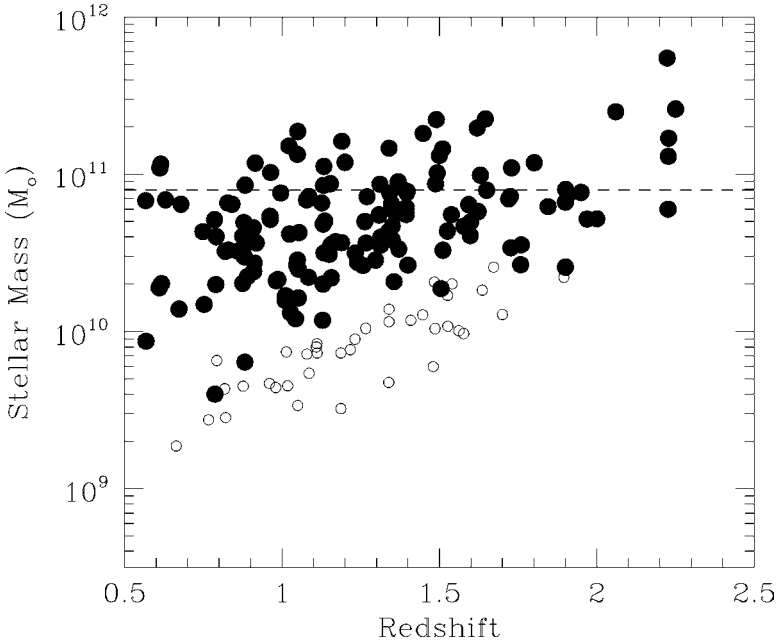


Figure 14 Stellar masses as a function of redshift from the GDDS (Glazebrook et al. 2004) and GOODS (Daddi et al. 2004) surveys: $K < 20$ = filled symbols; $K < 20.8$ = open symbols; present value of M^* from the 2MASS luminosity function by Cole et al. (2001) = dashed line.

at $z = 1.4$ that is a factor of 50 – 100 larger than that predicted by the Baugh et al. (2002) model. Recent semianalytic models by Somerville et al. (2004) come much closer to reproducing the observed mass density, but not the color distributions.

9. THE RED GALAXIES IN CONTEXT

One of the primary lessons from the first decade of studies of the faint red galaxies is that they are not a single population that conforms to any particular simple expectation. Perhaps it is not surprising that there is more than one route to this corner of color-magnitude space, but it is frustrating that we remain unable to characterize the mix of the two main constituents with satisfactory precision. This particular region of color-magnitude space awaited the detector advances of the 1980s and 1990s before any meaningful exploration could be carried out, and it will await the imminent space-IR and improved millimeter/submillimeter facilities before we can cleanly pry apart the various contributors. Early results are starting to appear at the time of this writing (e.g., Yan et al. 2004b); more will certainly appear while the present work is in press.

Many statistical inferences, however, can be drawn from the current data regarding the properties and evolution of the star-forming and passive components of the red population. The red star-forming galaxies clearly show that there is an important contributor to the star-formation history of the universe that is missed in the rest-UV-based census. The star-forming EROs may represent the extreme end of obscured star formation, whereas the total contribution of obscured star formation is likely to include a wide range of extinction levels. SCUBA and the Infrared Space Observatory (ISO) give us both clear evidence that this is the case and a preview of what is to come with *Spitzer*, The Large Atacama Millimeter Array (ALMA), and other facilities. The star-forming EROs suggest that a significant amount of star formation is hidden from the view of visible-wavelength astronomy and offers the tantalizing possibility that there is obscured star formation at very high redshifts awaiting discovery.

The passively evolving population of red galaxies are more difficult to place in context. It seems fairly certain that the redshift distributions and luminosity functions of passive red galaxies at $z > 1$ are in serious conflict with the hierarchical models and that at face value they point toward high formation redshifts for the spheroids. The degree of conflict between theory and observation here is uncertain because of the poorly known mix of passive and star-forming objects in the red samples, the difficulty in obtaining complete spectroscopic samples and the natural elasticity of theory. The existence of very massive galaxies at high redshift and the apparent lack of evolution of the mass function, while tentative, also favor early formation. The increased AGN activity in evolved galaxies at high redshift, seen both in the X rays and radio, and the correlation between black-hole mass and bulge properties today (Ferrarese & Merritt 2000, Gebhardt et al. 2000) argue that there is a long-lived connection between black holes and the spheroid population sampled by the passive red galaxies. The distant radio galaxies and the tight *K*-Band *Hubble* diagram also point toward an ancient origin for the cores of these systems.

If we are to postulate that the massive $1 < z < 2$ red galaxies formed in rapid collapse at high redshifts (e.g., ~ 5), then we must confront the apparent lack of progenitors. It is no longer possible to ignore the issue of detectability of classical primeval galaxy progenitors to the massive spheroids. Objects with star-formation rates of $1000 M_{\odot} \text{ yr}^{-1}$ at $z = 5$ are not easy to hide and, if unobscured, should have been detected in deep imaging and spectroscopic surveys (e.g., Dickinson et al. 2004). Thus we must ask if any of the known galaxy types at $z > 3$, the LBGs, faint Ly α emitters, and SCUBA sources, are suitable progenitors of the passive ERO population. The LBGs have the space density and star-formation rates needed to produce the present day spheroidal population (e.g., Steidel et al. 1999). It is less clear that they can produce the massive red population by $z \sim 2$. The large difference in clustering properties, the high stellar masses seen at $z > 1.5$ and apparently large ages at $z \sim 2$ (McCarthy et al. 2004) appear to argue for earlier or more vigorous star formation than the typical LBG, although the older component of the LBG population may have the required masses and ages. The clustering

difference remains and as this does not evolve rapidly, a large commonality between the LBGs and EROs appears unlikely. The red $J - K$ selected galaxies at $z > 2$ (Franx et al. 2003, van Dokkum et al. 2003) appear to be far closer analogs to the passive EROs at $z \sim 1$, and it is quite plausible that they form an evolutionary sequence. The question of progenitors remains, it simply moves from the $I - K$ to the $J - K$ -selected populations.

The only objects that we presently know of that reach both very high star-formation rates and high redshifts are the submillimeter sources. The most spectacular SCUBA-selected sources have star-formation rates of $1000 M_{\odot}$, sufficient to be classical primeval galaxies. At present one can identify SCUBA sources at $z \sim 2-3$ (e.g., Chapman et al. 2003). Whereas these objects may be progenitors of the $z \sim 1$ red galaxies, higher redshift analogs would be more appropriate progenitors for the $z \sim 2$ massive galaxies. The statistics of the SCUBA sources allow a minority population with redshifts beyond four. These have yet to be observed and are likely to constitute only a small fraction of the current SCUBA population.

If the ages of 53W091-like objects and the $z = 1.8$ GDDS objects can be pushed as short as 1 Gyr, then there may be no difficulty with the $z \sim 2-3$ SCUBA sources evolving into the $z \sim 1-2$ passive EROs. In this view the Arp220-like EROs may not be unrelated to the passive EROs as rapid merging and segregation of stars by phase space and the clearing of gas via galactic winds may be able to assemble old elliptical galaxies from merging spirals in a few dynamical times. Thus HR10 might evolve into an old ERO at $z = 1$. In this scenario the bulk of the mergers must happen before $z \sim 2$ to allow most of the stellar mass in the most massive galaxies to be in place at $z = 1.5$.

If the ages are closer to their apparently preferred values of ~ 3 Gyr then the progenitor population is pushed firmly into the Dark Ages epoch and thus may not be present in any of our current optical surveys. The diffuse IR backgrounds then provide the most stringent limits on a luminous population of early starbursts. As discussed above, Barger et al. (2003) argued that most of the $850 \mu\text{m}$ -background is in identified sources and thus cannot be at $z \gg 3$.

The red and blue galaxies present us with a number of interesting conundrums. The mass in the passive red population appears to be unevolving from $z \sim 2.5$ to the present, yet deep *HST* and LBG studies suggest that only 3–15% of the present stellar-mass density is present at $z = 2.7$ (Dickinson et al. 2004). Rapid evolution in the mass density is inferred in the $1 < z < 2.7$ period by Dickinson et al. (2004), yet Figure 14 implies that the high-mass galaxies experience only modest evolution in precisely this same interval. The masses and ages of the red galaxies naively demand an early epoch of intense star formation and galaxy building, yet none is seen at this time. Forming the stars early and building the galaxies slowly does not solve the problem of the masses and is thus not a solution unless it can be accomplished more rapidly than the current hierarchical models imply.

This is a high-risk review. Many of the issues raised by the properties of the red galaxies as inferred from optical to near-IR studies and shallow submillimeter to radio observations will be resolved while this volume is in press. Thus I can hope at

best to clearly outline the state of the field at this time. *Spitzer* will initiate a second decade of research into the processes that produce the faint red galaxies, and we can look forward to the next reviewer setting straight many of the conflicting ideas put forth here.

ACKNOWLEDGMENTS

I thank Hsiao-Wen Chen for her many helpful contributions, particularly with the figures. I am grateful to Anne Sheldon and Veronica Padilla for their work in making this into a readable article. Finally I thank Alan Sandage and Eric Persson for careful readings of the text and many helpful suggestions.

**The Annual Review of Astronomy and Astrophysics is online at
<http://astro.annualreviews.org>**

LITERATURE CITED

- Abraham RG, Glazebrook K, McCarthy PJ, Crampton DC, Roth K, et al. 2004. *Ap. J.* 127:245
- Afonso J, Hopkins AM, Sullivan M, Mobasher B, Georgakakis A, Cram LE. 2003. In *Multiwavelength Mapping of Galaxy Formation and Evolution*. Garching, Ger.: ESO
- Alexander DM, Bauer FE, Brandt WN, Schneider DP, Hornschemeier AE, et al. 2003. *Astron. J.* 126:539
- Alexander DM, Vignall C, Bauer FE, Brandt WN, Hornschemeier AE, et al. 2002. *Astron. J.* 123:1149
- Andreani P, Cimatti A, Loinard L, Rottgering HJA. 2000. *Astron. Astrophys.* 354:L1
- Barger AJ, Cowie LL, Capak P, Alexander DM, Bauer FE, et al. 2003. *Astron. J.* 126:632
- Barger AJ, Cowie LL, Richards EA. 2000. *Astron. J.* 119:2092
- Barger AJ, Cowie LL, Threntham N, Fulton E, Hu EM, et al. 1999. *Astron. J.* 117:102
- Baugh CM, Benson AJ, Cole S, Frenk CS, Lacey C. 2003. In *The Mass of Galaxies at Low and High Redshift*, Proc. ESO Workshop, p. 91, Venice, Italy, Oct. 2001. Germany: ESO
- Bell EF, McIntosh DH, Katz N, Weinberg MD. 2003a. *Ap. J. Suppl.* 149:289
- Bell EF, Wolf C, Meisenheimer K, Rix H-W, Borch A, et al. 2004. *Ap. J.* In press. (astro-ph 0303394)
- Bergstrom S, Wiklind T. 2004. *Astron. Astrophys.* 414:95
- Brandt WN, Alexander DM, Hornschemeier AE, Garmire GP, Schneider DP, et al. 2001. *Astron. J.* 122:2810
- Brinchmann J, Ellis RS. 2000. *Ap. J.* 536:77
- Brown MJ, Dey A, Jannuzi BT, Lauer TR, Tiede GP, Mikles VJ. 2003. *Ap. J.* 597:225
- Brusa M, Comastri A, Daddi E, Cimatti A, Mignoli M, Pozzetti L. 2002. *Ap. J.* 581:L89
- Bruzual G, Magris GC. 1997. In *The Ultraviolet Universe at Low and High Redshift: Probing the Progress of Galaxy Evolution*. AIP Conf. Proc. 408:291
- Budavri T, Connolly AJ, Szalay AS, Szapudi I, Csabai I, et al. 2003. *Ap. J.* 595:59
- Carilli CL, Yun MS. 2000. *Ap. J.* 539:1024
- Chapman S, McCarthy P, Persson SE. 2000. *Astron. J.* 120:1612
- Chapman SC, Blain AW, Ivison RJ, Smail IR. 2003. *Nature* 422:695
- Chen H-W, Marzke R, McCarthy PJ, Martini P, Carlberg RG, et al. 2003. *Ap. J.* 586:745
- Chen HW, McCarthy PJ, Marzke RO, Wilson J, Carlberg RG, et al. 2002. *Ap. J.* 570:54
- Chen HW, LCIRS Team, GDDS Team. 2004. In *Multiwavelength Mapping of Galaxy*

- Formation and Evolution*. Garching, Ger.: ESO. In press
- Cimatti A. 2003a. In *Galaxy Evolution: Theory & Observations*, ed. V Avila-Reese, C Firmani, CS Frenk, C Allen, 17:209–13. Rev. Mex. Astro. Astrofis. (Ser. Conf.)
- Cimatti A. 2003b. In *The Mass of Galaxies at Low and High Redshift*. Proc. ESO Workshop, Venice, Italy, Oct. 2001, ESO, p. 124
- Cimatti A, Daddi E, Cassata P, Pignatelli E, Fasano G, et al. 2003. *Astron. Astrophys.* 412:1
- Cimatti A, Andreani P, Rottgering H, Tilanus R. 1998. *Nature* 392:895
- Cimatti A, Daddi E, di Serego Alighieri S, Moriondo G, Pozzetti L, et al. 2000. *SPIE* 4005:54
- Cimatti A, et al. 2004. *Astron. Astrophys.* In press. (astro-ph 0310742)
- Cimatti A, Daddi E, Mignoli M, Pozzetti L, Renzini A, et al. 2002a. *Astron. Astrophys.* 381:L68
- Cimatti A, Pozzetti L, Mignoli M, Daddi E, Menci N, et al. 2002b. *Astron. Astrophys.* 391:L1
- Cohen JG, Hogg DW, Blandford R, Cowie LL, Hu E, Songail A, Shopbel P, Richberg K. 2000. *Ap. J.* 528:39
- Colbert EJM, Mushotzky RF. 1999. *Ap. J.* 519:89
- Cole S, Lacey CG, Baugh CM, Frenk CS. 2000. *MNRAS* 319:168
- Cole S, Nordberg P, Baugh CM, Frenk CS, Bland-Hawthorn J, et al. 2001. *MNRAS* 326:255
- Coleman GD, Wu C-C, Weedman DW. 1980. *Ap. J.* (Suppl.)43:393
- Cowie LL, Gardner JP, Lilly SJ, McLean I. 1990. *Ap. J.* 360:L1
- Cowie LL, Hu E, Songaila A. 1995. *Astron. J.* 110:1576
- Daddi E, Cimatti A, Renzini A, Vernet J, Conselice C, et al. 2004. *Ap. J.* 600:127
- Daddi E, Cimatti A, Broadhurst T, Renzini A, Zamorani G, et al. 2002. *Astron. Astrophys.* 384:L1
- Daddi E, Cimatti A, Pozzetti L, Hoekstra H, Rottgering H, et al. 2000. *Astron. Astrophys.* 361:535
- Daddi E, Cimatti A, Renzini A. 2001. *Astron. Astrophys.* 362:L45
- Dey A, Graham JR, Ivison R, Smail I, Wright G, Lui M. 1999. *Ap. J.* 519:610
- de Breuck C, van Breugel W, Stanford A, Rottgering H, Miley G, Stern D. 2003 In *The Mass of Galaxies at Low and High Redshift*, Proc. ESO Workshop, Venice, Italy, Oct. 2001, ESO, p. 156
- Dickinson M, Stern D, Giavalisco M, Ferguson HC, Tsvetanov Z, et al. 2004. *Ap. J.* 600:99
- Dickinson M, Papovich C, Ferguson HC, Budavari T. 2003. *Ap. J.* 587:25
- Djorgovski S, Soifer BT, Pahre MA, Larkin JE, Smith JD, et al. 1995. *Ap. J.* 438:13
- Dunlop J, Peacock J, Spinrad H, Dey A, Jimenez R, et al. 1996. *Nature* 381:581
- Dunlop JS, Peacock JA, Savage A, Lilly SJ, Heasley JN, Simon AJB. 1989. *MNRAS* 238:1171
- Eggen OJ, Lynden-Bell D, Sandage AR. 1962. *Ap. J.* 136:748
- Eisenstein DJ, Hogg DW, Fukugita M, Nakamura O, Bernardi M, et al. 2003. *Ap. J.* 585:694
- Elbaz D, Flores H, Chantal P, Mirabel IF, Sanders D, et al. 2002. *Astron. Astrophys.* 381:L1
- Ellis RS, Colless M, Broadhurst T, Heyl J, Glazebrook K. 1996. *MNRAS* 280:253
- Elston R, Rieke GH, Rieke MJ. 1988. *Ap. J.* 331:L77
- Elston R, Rieke GH, Rieke MJ. 1989. *Ap. J.* 341:L80
- Ferrarese L, Merritt D. 2000. *Ap. J.* 539:L9
- Fioc M, Rocca-Volmerange B. 1997. *Astron. Astrophys.* 326:95
- Firth AE, Somerville RS, McMahon RG, Lahav O, Ellis RS, et al. 2001. *MNRAS* 332:617
- Fontana A, Pozzetti L, Donnarumma I, Renzini A, Cimatti A, et al. 2004. *Astron. Astrophys.* In press. (astro-ph/0405055)
- Franceschini A, Silva L, Fasano Gi, Granato GL, Bressan A, Arnouts S, Danese L. 1998. *Ap. J.* 506:600

- Franx M, Labbe I, Rudnick G, van Dokkum PG, Daddi E, et al. 2003. *Ap. J.* 587:L79
- Frayer DT, Armus L, Scoville NZ, Blain AW, Reddy NA, Ivison RJ, Smail I. 2003. *Astron. J.* 126:73
- Gardner JP, Sharples RM, Carrasco BE, Frenk CS. 1996. *MNRAS* 282:1
- Gebhardt K, Bender R, Bower G, Dressler A, Faber SM, et al. 2000. *Ap. J.* 539:L13
- Giacconi R, Rosati P, Tozzi P, Nonino M, Hasinger G. 2001. *Ap. J.* 551:624
- Giavalisco M. 2002. *Annu. Rev. Astron. Astrophys.* 40:579
- Giavalisco M, Dickinson M. 2001. *Ap. J.* 550:177
- Giavalisco M, Steidel CC, Adelberger KL, Dickinson ME, Pettini M, Kellogg M. 1998. *Ap. J.* 503:543
- Gilbank D, Smail I, Ivison R, Packham C. 2004. *MNRAS* 346:1125
- Glazebrook K, Abraham RG, McCarthy PJ, Savaglio S, Chen H-W, et al. 2004. *Nature*. In press
- Guzzo L, Strauss MA, Fisher KB, Giovanelli R, Haynes MP. 1997. *Ap. J.* 489:37
- Graham JR, Dey A. 1996. *Ap. J.* 471:720
- Greve TR, Ivison RJ, Papadopoulos PP. 2003. *Ap. J.* 599:839
- Griffiths RE, Ratnatunga KU, Neuschaefer LW, Casertano S, Im M, et al. 1994. *Ap. J.* 437:67
- Holland WS, Robson EI, Gear WK, Cunningham CR, Lightfoot JF, et al. 1999. *MNRAS* 303:659
- Hu E, Ridgeway S. 1994. *Astron. J.* 107:1303
- Huang J-S, Thompson D, Kummel WM, Meisenheimer K, Wolf C, et al. 2001. *Astron. Astrophys.* 368:787
- Im M, Griffiths RE, Ratnatunga KU, Sarajedini VL. 1996. *Ap. J.* 461:79
- Im M, Yamada T, Tanaka I, Kajisawa M. 2002. *Ap. J.* 578:L19
- Jannuzi BT, Dey A, Brown MJI, Tiede GP, et al. 2004. *Bull. Am. Astron. Soc.* 34:1271
- Jimenez R, Friaca ACS, Dunlop JS, Terlevich RJ, Peacock JA, Nolan LA. 1999. *MNRAS* 305:151
- Johnson H. 1962. *Ap. J.* 135:69
- Jorgensen I, Franx M, Hjorth J, van Dokkum PG. 1999. *MNRAS* 308:833
- Kauffmann G, Colberg JM, Diaferio A, White SDM. 1999. *MNRAS* 307:529
- Kauffmann G, Charlot S. 1998. *MNRAS* 297:L23
- Kauffmann G, Charlot S, White SDM. 1996. *MNRAS* 283:117
- Kauffmann G, Colber JM, Diaferio A, White SDM. 1999. *MNRAS* 307:529
- Kauffman G, Heckman TM, White SDM, Charlot S, Tremonti C, et al. 2003. *MNRAS* 341:33
- Kochanek CS, Pahre MA, Falco EE, Huchra JP, et al. 2001. *Ap. J.* 560:566
- Laing RA, Riley JM, Longair MS. 1983. *MNRAS* 204:151
- Lilly SJ, Le Fevre O, Crampton D, Hammer F, Tresse L. 1995a. *Ap. J.* 455:50
- Lilly SJ, Longair MS. 1984. *MNRAS* 211:833
- Lilly SJ, Tresse L, Hammer F, Crampton D, Le Fevre O. 1995b. *Ap. J.* 455:108
- Limber DN. 1953. *Ap. J.* 117:134
- Lubin L, Sandage A. 2001. *Astron. J.* 122:1084
- Madau P, Ferguson HC, Dickinson ME, Giavalisco M, Steidel CC, Fruchter A. 1996. *MNRAS* 283:1388
- Martini P. 2001. *Astron. J.* 121:2301
- McCarthy P. 1993. *Annu. Rev. Astron. Astrophys.* 31:639–88
- McCarthy PJ, Carlberg RG, Chen W-H, Marzke RO, First AE, et al. 2001. *Ap. J.* 560:L131
- McCarthy PJ, Crampton D, Le Borgne D, Chen H-W, Abraham RG, et al. 2004. *Ap. J.* Submitted
- McCarthy PJ, Persson SE, West SC. 1992. *Ap. J.* 386:52
- Menci N, Cavaliere A, Fontana A, Giallongo E, Poli F. 2002. *Ap. J.* 575:18
- Mohan NR, Cimatti A, Rottgering HJA, Andreani P, Severgnini P, et al. 2002. *Astron. Astrophys.* 383:440
- Moriondo G, Cimatti A, Daddi E. 2000. *Astron. Astrophys.* 364:26
- Moustakas LA, Davis M, Graham JR, Silk J, Peterson BA, Yoshii Y. 1997. *Ap. J.* 475:445
- Moustakas LA, Casertano S, Conselice CJ,

- Dickinson ME, Eisenhardt P, et al. 2004. *Ap. J.* 600:131
- Nolan LA, Dunlop JS, Jimenez R. 2001. *MNRAS* 323:385
- Ouchi M, et al. 2004. *Ap. J.* In press
- Papovich C, Dickinson M, Ferguson HC. 2001. *Ap. J.* 559:620
- Peacock JA, Nicholson D. 1991. *MNRAS* 253:307
- Peebles PJE. 1980 *Principles of Physical Cosmology*, Princeton University Press. 217 pp.
- Persson SE, McCarthy PJ, Dressler A, Matthews K. 1993. In *The Evolution of Galaxies and Their Environments. NASA Conf. 78:79*
- Pierini D, Maraston C, Bender R, Witt AN. 2004. *MNRAS* 347:1
- Poggianit BM. 1997. *Astron. Astrophys.* 122:399
- Pozzetti L, Cimatti A, Zamorani G, Daddi E, Menci N, et al. 2003. *Astron. Astrophys.* 402:837
- Pozzetti L, Madau P, Zamorani G, Ferguson HC, Bruzual G. 1998. *MNRAS* 298:1133
- Pozzetti L, Mannucci F. 2000. *MNRAS* 317:17
- Pozzetti L, Zamorani G, Bruzual AG. 1996. In *From Stars to Galaxies: The Impact of Stellar Physics on Galaxy Evolution. ASP Conf.* 98:588
- Rieke GH, Cutri RM, Black JH, Kailey WF, McAlary CW, et al. 1985. *Ap. J.* 290:116
- Rosati P, Tozzi P, Giacconi R, Gilli R, Hasinger G, et al. 2002. *Ap. J.* 566:667
- Rudnick G, Rix H-W, Franx M, Labbe I, Blanton M, et al. 2003. *Ap. J.* 599:847
- Sandage A. 1986. *Astron. Astrophys.* 161:89
- Sandage A. 1990. *J. R. Astron. Soc. Canada* 84:70
- Saracco P, Longhetti M, Severgnini P, Della Ceca R, Bender R, et al. 2003. In *Galaxy Evolution: Theory and Observation*, ed. V Avila-Reese, C Firmani, CS Frenk, C Allen, 17:249. Rev. Mex. Astron. Astrofis. (Ser. Conf.)
- Schechter PL, Dressler A. 1987. *Astron. J.* 94:563
- Scodreggio M, Silva DR. 2000. *Astron. Astrophys.* 359:953
- Searle L, Zinn R. 1978. *Ap. J.* 223:82
- Shapley AE, Steidel CC, Adelberger KL, Dickinson ME, Giavalisco M, Petinni M. 2001. *Ap. J.* 562:95
- Smail I, Ivison RJ, Kneib J-P, Cowie LL, Blain AW, et al. 1999. *MNRAS* 308:1061
- Smail I, Owen FN, Morrison GE, Keel WC, Ivison RJ, Ledlow MJ. 2002. *Ap. J.* 581:844
- Smith GP, Smail I, Kneib J-P, Czoske O, Ebling H, et al. 2002. *MNRAS* 330:1
- Soifer BT, Matthews K, Neugebauer G, Armus L, Cohen JG, et al. 1999. *Astron. J.* 118:2065
- Somerville RS, Primack JR. 1999. *MNRAS* 310:1087
- Somerville RS, Primack JR, Faber S. 2001. *MNRAS* 320:504
- Somerville RS, Moustakas LA, Mobasher B, Gardner JP, Cimatti A, et al. 2004. *Ap. J.* 600:171
- Songaila A, Cowie LL, Hu EM, Gardner JP. 1994. *Ap. J. Suppl.* 94:461
- Spinrad H, Dey A, Stern D, Dunlop J, Peacock J, et al. 1997. *Ap. J.* 484:581
- Stanford SA, Dickinson M, Postman M, Ferguson HC, Lucas RA, Conselice CJ, Budavari T, Somerville R. 2004. *Astron. J.* 127, 131
- Stanford SA, Eisenhardt PR, Dickinson M. 1995. *Ap. J.* 450:512
- Stanford SA, Eisenhardt PR, Dickinson M. 1998. *Ap. J.* 492:461
- Stevens JA, Page MJ, Ivison RJ, Smail I, Lehmann I, et al. 2003. *MNRAS* 342:249
- Stiavelli M, Treu T. 2001. In *Galaxy Disks and Disk Galaxies*, ASP Conf. Ser., pp. 603–6
- Steidel C, Adelberger K, Giavalisco M, Dickinson M, Pettini M. 1999. *Ap. J.* 519:1
- Steidel CC, Dickinson M, Persson SE. 1994. *Ap. J.* 437:75
- Takata T, Kashikawa N, Nakanishi K, Aoki K, Asai R, et al. 2003. *PASJ* 55:789
- Thompson D. 1999. In *Astrophysics with Infrared Surveys: A Prelude to SIRTf*, ASP Conference Series, Vol. 177. Ed. Michael D. Bicay, Roc M. Cutri, and Barry F. Madore. p. 51
- Thompson D, Beckwith SVW, Fockenbrock R, Fried J, Hippelein H, et al. 1999. *Ap. J.* 523:100

- Treu T, Stiavelli M. 1999. *Ap. J.* 524:L27
- van der Wel A, Franx M, van Dokkum PG, Rix H-W. 2004. *Ap. J.* 601:5
- van Dokkum PG, Stanford SA. 2003. *Ap. J.* 585:78
- van Dokkum PG, Forster S, Natascha M, Franx M, Daddi E, et al. 2003. *Ap. J.* 587:L83
- Wainscoat RJ, Cowie LL. 1992. *Astron. J.* 103:332
- Wehner EH, Barger AJ, Knieb J-P. 2002. *Ap. J.* 577:L83
- Willmer CNA, da Costa LN, Pellegrini PS. 1998. *Astron. J.* 116:1
- Windhorst RA, van Heerde GM, Katgert P. 1984. *Astron. Astrophys.* 58:1
- Wolf C, Meisenheimer K, Rix H-W, Borch A, Dye S, Kleinheinrich M. 2003. *Astron. Astrophys.* 401:73
- Yan L, McCarthy PJ, Weymann RJ, Malkan MA, Teplitz HI, et al. 2000. *Astron. J.* 120:575
- Yan L, McCarthy PJ, Storrie-Lombardi LJ, Weymann RJ. 1998. *Ap. J.* 503:19
- Yan L, Thompson D. 2003. *Ap. J.* 586:765
- Yan L, Thompson D, Soifer BT. 2004. *Astron. J.* 127:1274
- Yi S, Brown TM, Heap S, Hubeny I, Landsman W, et al. 2000. *Ap. J.* 533:670
- Yun MS, Carilli CL. 2002. *Ap. J.* 568:88
- Zehavi I, Blanton MR, Frieman JA, Weinberg DH, Mo HJ, et al. 2002. *Ap. J.* 571:172
- Zepf S. 1997. *Nature* 390:377

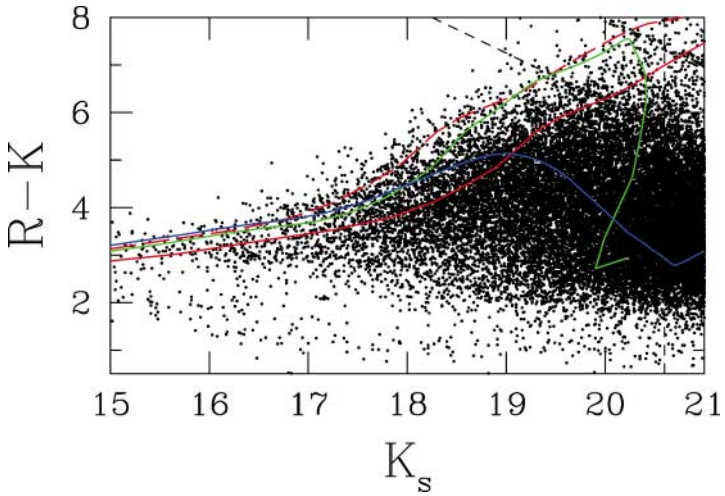


Figure 4 A modern $R - K$ versus K color-magnitude diagram from the Las Campanas IR Survey. The red envelope is well-defined from large area surveys and the declining numbers of objects as a function of color is clearly discerned. It is of interest to compare Figures 3 and 4. The Elston et al. (1988) field selection, shown in Figure 3, was quite unrepresentative, $R - K \sim 5$ objects with $K \sim 16.5$ are quite rare. Tracks for no evolution and $\tau = 1$ Gyr with $z_f = 10$ and 5 are shown.

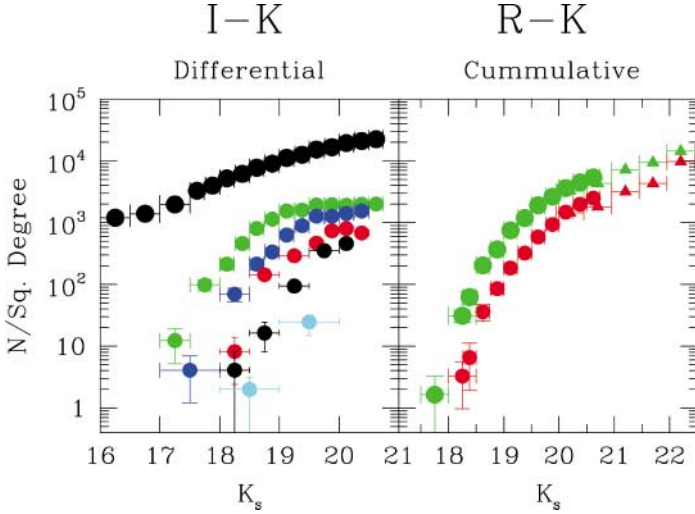


Figure 5 Counts of K -selected and color-defined samples. The left panel shows differential number counts for galaxies selected on the basis of $I - K$ color. The upper (*black*) points are the full K -selected sample, the lower curves show galaxies with color ranges from 3.5–4.0 (*green*), 4.0–4.5 (*blue*), 4.5–5.0 (*red*), 5.0–5.5 (*black*), and >5.5 (*cyan*). The right panel shows cumulative counts for galaxies defined by $R - K > 5.3$ (*green*) and >6.0 (*red*). In both plots the circular symbols are data from the LCIR survey (McCarthy et al. 2001); the triangles in the right panel are data from Smith et al. (2002).

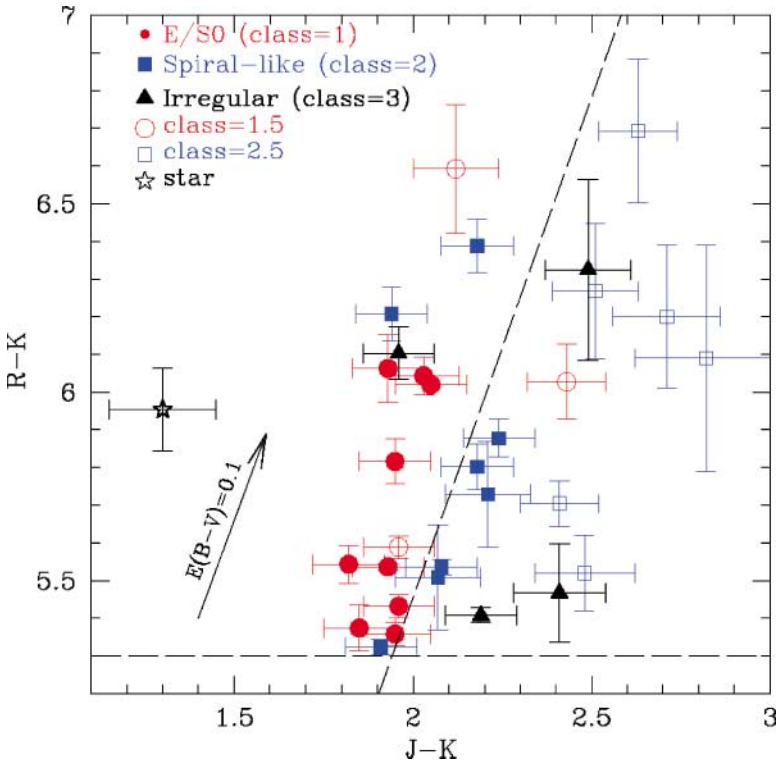


Figure 6 The two-color $R - K$ versus $J - K$ diagram from Cimatti et al. (2003c). The symbols reflect the authors classification of the objects by Cimatti et al. (2003c) on the basis of their morphologies and spectral types. The dashed lines demark the division between passive (*left*) and reddened (*right*) systems.

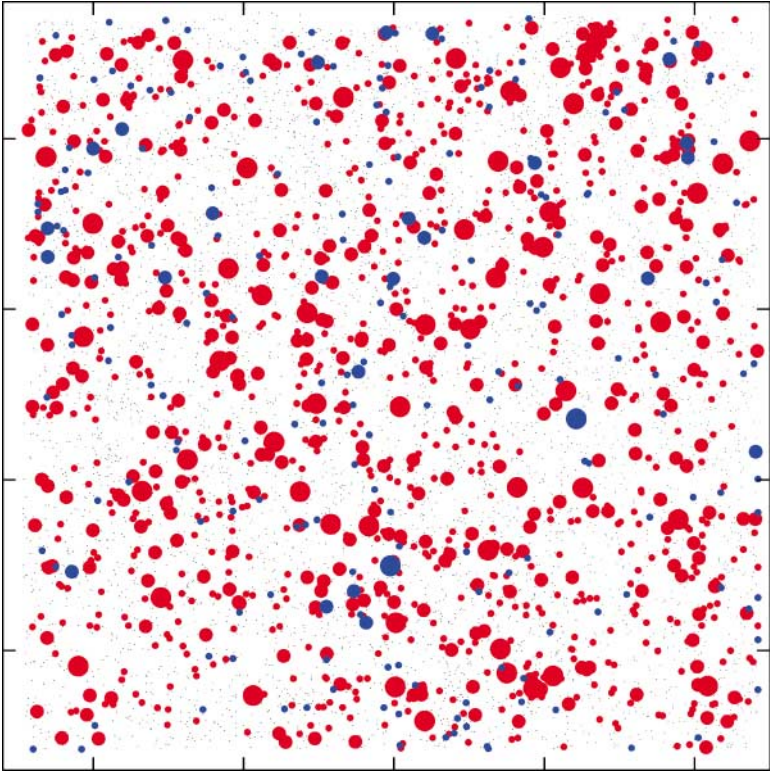


Figure 9 A map of a $26' \times 26'$ region of the sky from the LCIR survey showing the clustering of the red galaxies. The small black points are the complete $K < 20.6$ sample, the red and blue points are galaxies with $I - K > 4$ and $I - K > 5$, respectively. The size of the colored points is in proportion to their magnitudes in three steps: $K < 18$ (largest), $K < 19$, and $K < 20.6$ (smallest). The ticks marks on the border are in intervals of 0.1 degree and project to comoving scales of 0.5 Mpc at $z = 1$.

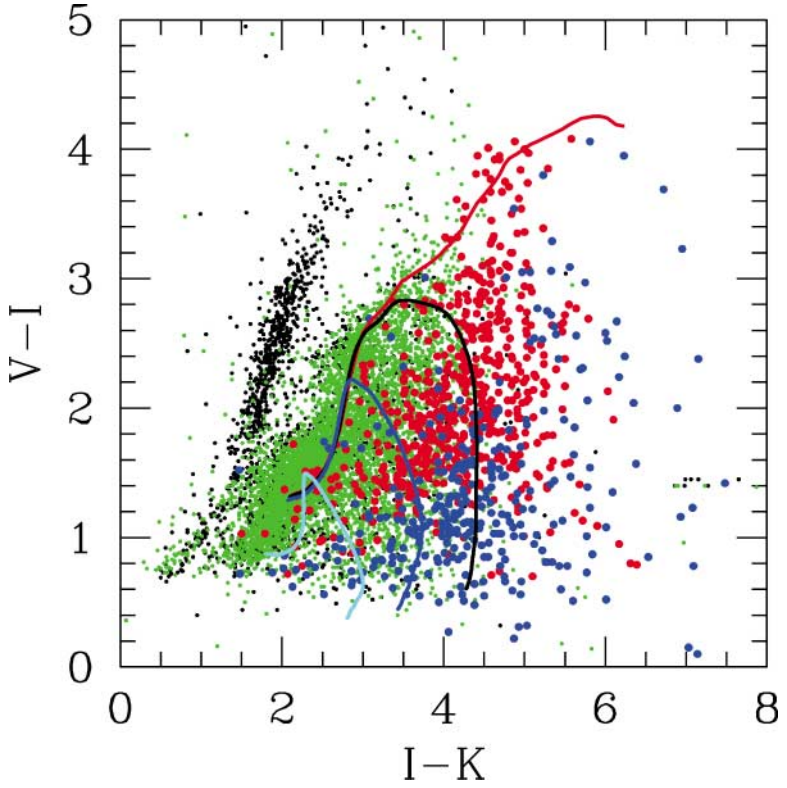


Figure 11 The two-color $V - I$ versus $I - K$ diagram for the $26' \times 26'$ CDFS field of the LCIR survey. The points are color coded by photometric redshift: black = stars, green = $z < 1$, red = $1 < z < 1.5$, and blue = $z > 1.5$. The stellar locus is clearly separated in this two-color projection. The curves are PEGASE2 models with $z_f = 20$ and e-folding times of 1 (red), 2 (black), and 3 (blue). A constant star-formation model is show in cyan. This diagram shows the diversity of UV colors at red $I - K$ colors and the apparent blueing of the rest-frame UV colors at high redshifts.

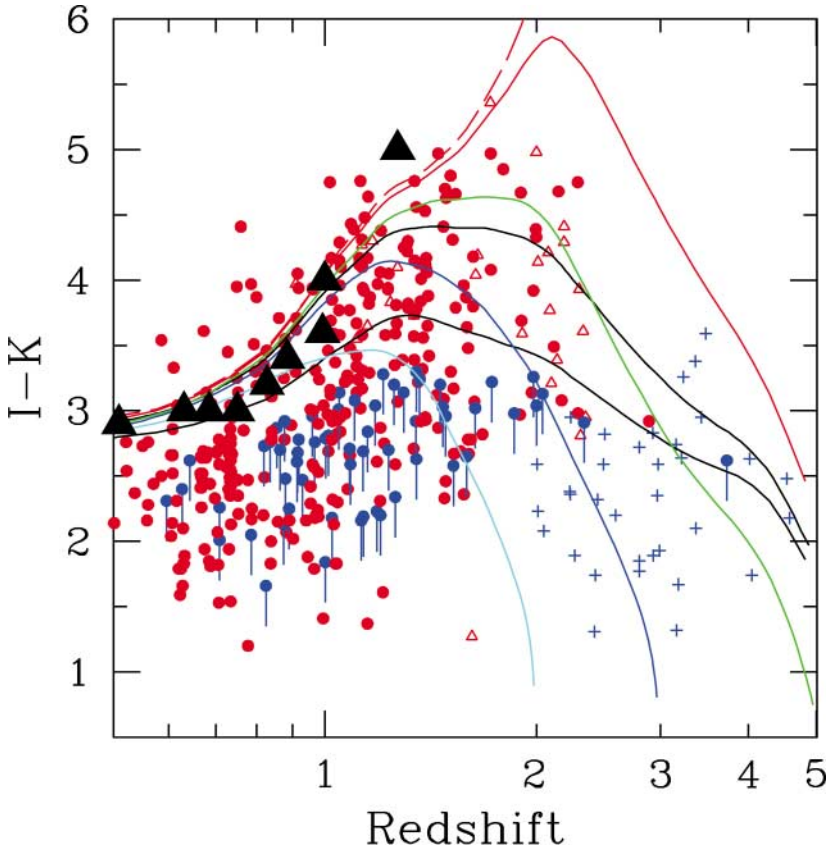


Figure 12 $I - K$ color versus redshift for the GDDS and LCIR samples. The red points have $K < 20.6$. The filled blue points are photo-z-selected objects with $K > 20.8$. The blue crosses are LBGs from the HDF-N with photometry from Papovich et al. (2001). The filled triangles show the $I - K$ color at K^* for the red sequences of clusters as measured by Stanford et al. (1995, 1998) and Chapman, McCarthy, & Persson (2000). The black curves are PEGASE2 (Fioc & Rocca-Volmerange 1997) models with $z_f = 30$ and decaying star-formation rates with e-folding times of 1 and 2 Gyr. The colored curves are 0.5 Gyr exponential PEGASE2 models with $z_f = 2$ (cyan), 3 (blue), 5 (green), and 10 (red). The red galaxy samples are nearly overlapping the low redshift end of the LBG samples. Of particular interest is the degree to which the red envelope population traces the expectations of early formation models and tracks the cluster locus (black triangles).

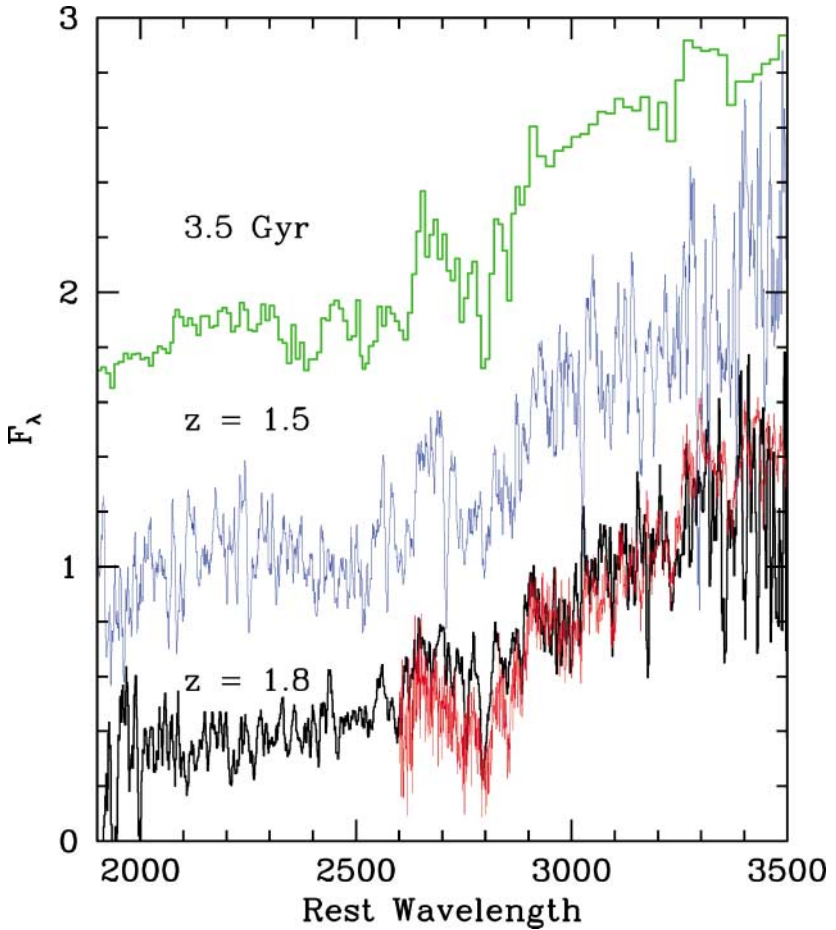


Figure 13 Spectra of the evolved galaxies at $z > 1.5$. The center spectrum is 53W091 from Dunlop et al. (1996), the lower spectrum is a composite of five galaxies with $1.6 < z < 1.9$ from the GDDS. The upper spectrum is a PEGASE2 (Fioç & Rocca-Volmerange 1997) spectral synthesis model with an age of 3.5 Gyr. The SDSS luminous red galaxy composite is overlaid on the red end of the GDDS $z = 1.8$ composite.